THE FEASIBILITY OF UTILIZING REMOTELY SENSED DATA TO ASSESS AND MONITOR OCEANIC GAMEFISH

M-8

by

Kenneth J. Savastano and Thomas D. Leming
National Marine Fisheries Service
Bay Saint Louis, Mississippi 39520

ABSTRACT

An investigation was conducted to establish the feasibility of utilizing remotely sensed data acquired from aircraft and satellite platforms to provide information concerning the distribution and abundance of oceanic gamefish. The investigation is currently in its analysis phase. The data from the test area was jointly acquired by NASA, the Navy, the Air Force and NOAA/NMFS elements and private and professional fishermen in the northeastern Gulf of Mexico. The data collected has made it possible to identify fisheries significant environmental parameters for white marlin. Prediction models, based on catch data and surface truth information, have been developed and have demonstrated a potential for significantly reducing search by identifying areas that have a high probability of productivity. Three of the parameters utilized by the models, chlorophyll-a, sea surface temperature and turbidity were inferred from aircraft sensor data and have been tested. Effective use of Skylab data was inhibited by cloud cover and delayed delivery. Initial efforts toward establishing the feasibility of utilizing remotely sensed data to assess and monitor the distribution of oceanic gamefish has successfully identified fisheries significant oceanographic parameters and demonstrated the capability of remotely measuring most of the parameters.

INTRODUCTION

An oceanic gamefish investigation was initiated in April 1973 with the primary objective of determining the feasibility of utilizing remotely sensed data acquired from aircraft and satellite platforms to assess and monitor the distribution of oceanic gamefish. The project was contracted to the National Marine Fisheries Services (NMFS) Fisheries Engineering Laboratory (FEL) by the National Aeronautics and Space Administration (NASA) Lyndon B. Johnson Space Center (JSC). Many elements of the National Oceanic and Atmospheric Administration (NOAA), the Air Force, the Navy, NASA, as well as numerous professional and sports fishermen participated in the investigation. This joint effort was undertaken to acquire fishery and oceanographic data in association with near simultaneously acquired Skylab - 3 and aircraft remotely sensed environmental data. This paper presents a summary of the results of the investigation. Earlier papers (1)(2) described the field operations and preliminary results of the August 4 and 5 investigation. Another report (3) describes the remote sensing of Oceanic Parameters during the Skylab Gamefish experiment. A complete report of the investigation and its analysis is scheduled to be completed in June 1975.

TARGET RESOURCE

The target resource of this investigation, oceanic gamefish, included billfishes, dolphin, wahoo,

and certain of the tunas. These gamefish constitute a major source of recreation for an increasing number of salt water anglers. In addition to the increasing domestic pressure, the resource is being exploited by the Japanese longline fishery and there are indications (4) that the fishing intensity has reached or exceeded the level beyond which a maximum annual yield cannot be sustained. This and other resource investigations will hopefully provide valuable information for the application of new management techniques to protect the resource.

TEST AREA

The test area (Figure 1) comprised 18000 square kilometers and was shaped roughly like a triangle, bounded by the coordinates 30° 16'N, 86° 51'W; 29° 18'N, 85° 47'W; and 29° 21'N, 87° 56'W on the north, east, and west respectively. The northern apex was 14 kilometers south of Santa Rosa Island and the southern serrated edge extended 155 km south of the apex. The sides extending from the northern apex approximated the 55 meters curve along the coast. The northern extremity of the De Soto Canyon lay within the southern portion of the area providing depths in excess of 1600 meters. In order to provide a grid for referencing gamefish catches, the fishing area was divided into 54 squares with 18.3 km (10 nautical miles) to a side. Skylab track 62 approximately bisected the area, extending southeast from Mobile Bay.

The test area is noted for an abundance of oceanic gamefish during the summer season. Numerous marinas are located along the coast line. Several gamefishing clubs are headquartered in nearby coastal cities and charter boat gamefishing is a viable industry in the coast economy. Figure 2 depicts an operational overview of the test area.

FIELD OPERATIONS AND DATA ACQUISITION

Skylab EREP Imagery

The Skylab Earth Resources Experiment Package (EREP) overpass occurred at approximately 1140 CDT on August 5 with 40 to 70 percent scattered cumulus cloud cover below 3000 meters. Duration of the overpass was about 40 seconds as the satellite transited southeasterly over the test side from the direction of Mobile Bay. The sensors activated during the overpass are shown with their respective applications for the project in Table I.

Aircraft Imagery

Aircraft data gathering missions were flown in the area on the morning of 5 August. A NASA earth survey aircraft, the NC130B, based in Houston, Texas, flew three flight lines totaling 413 km through the area at 6100 meters altitude. A contract light aircraft flew transects totaling 413 km at 3000 meters altitude. The aircraft sensor coverage is given in Table II.

Gamefish Data

A committee of representatives from six gamefishing clubs and charterboat associations headquartered in Alabama, Florida, and Louisiana, coordinated the volunteer fishing program to acquire data on the living marine resource. These data were acquired through a Skylab Gamefish Tournament held August 4-5 under the general management of the Pensacola Big Game Fishing Club.

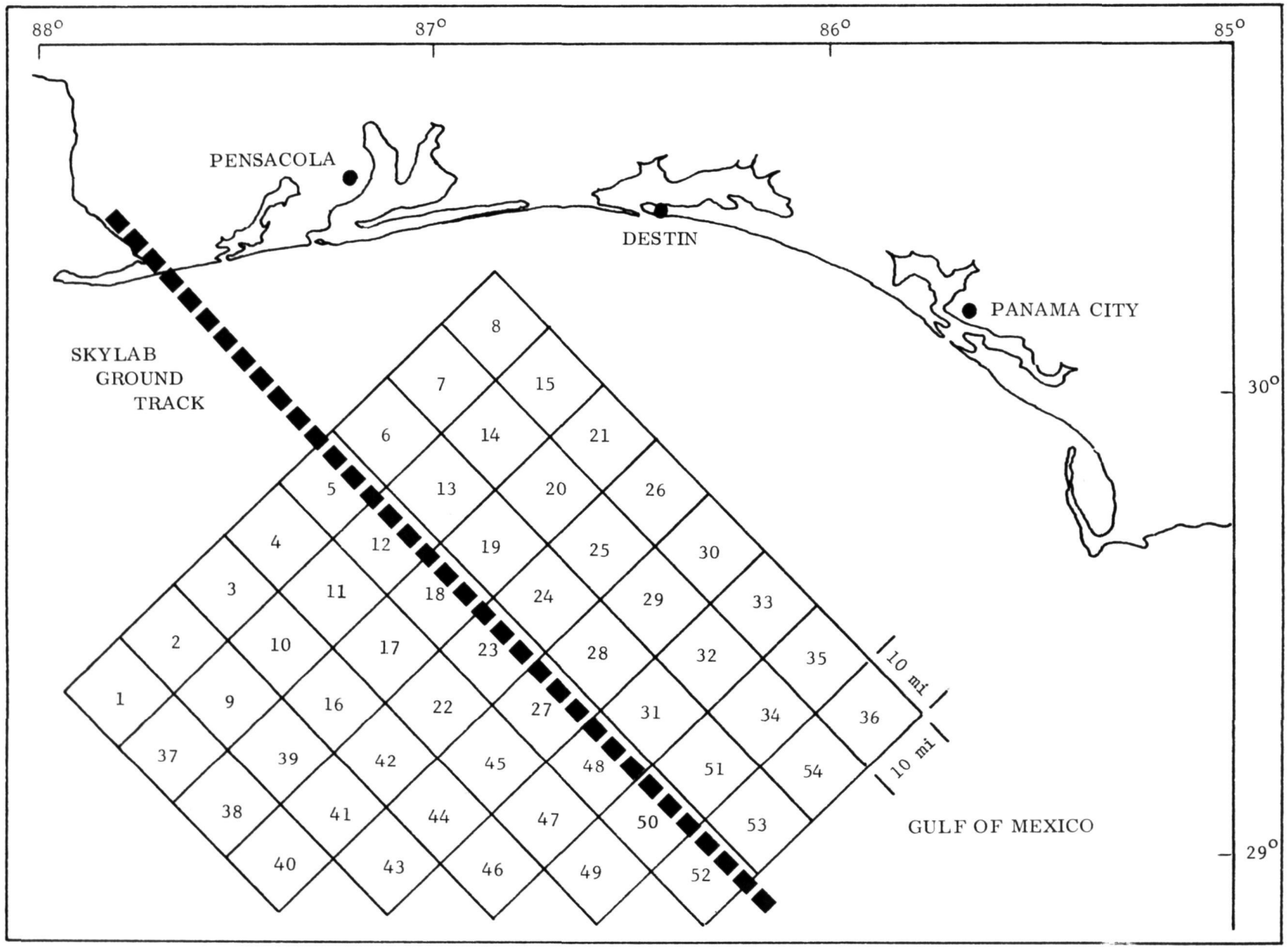

Figure 1. Test Area With Fishing Squares

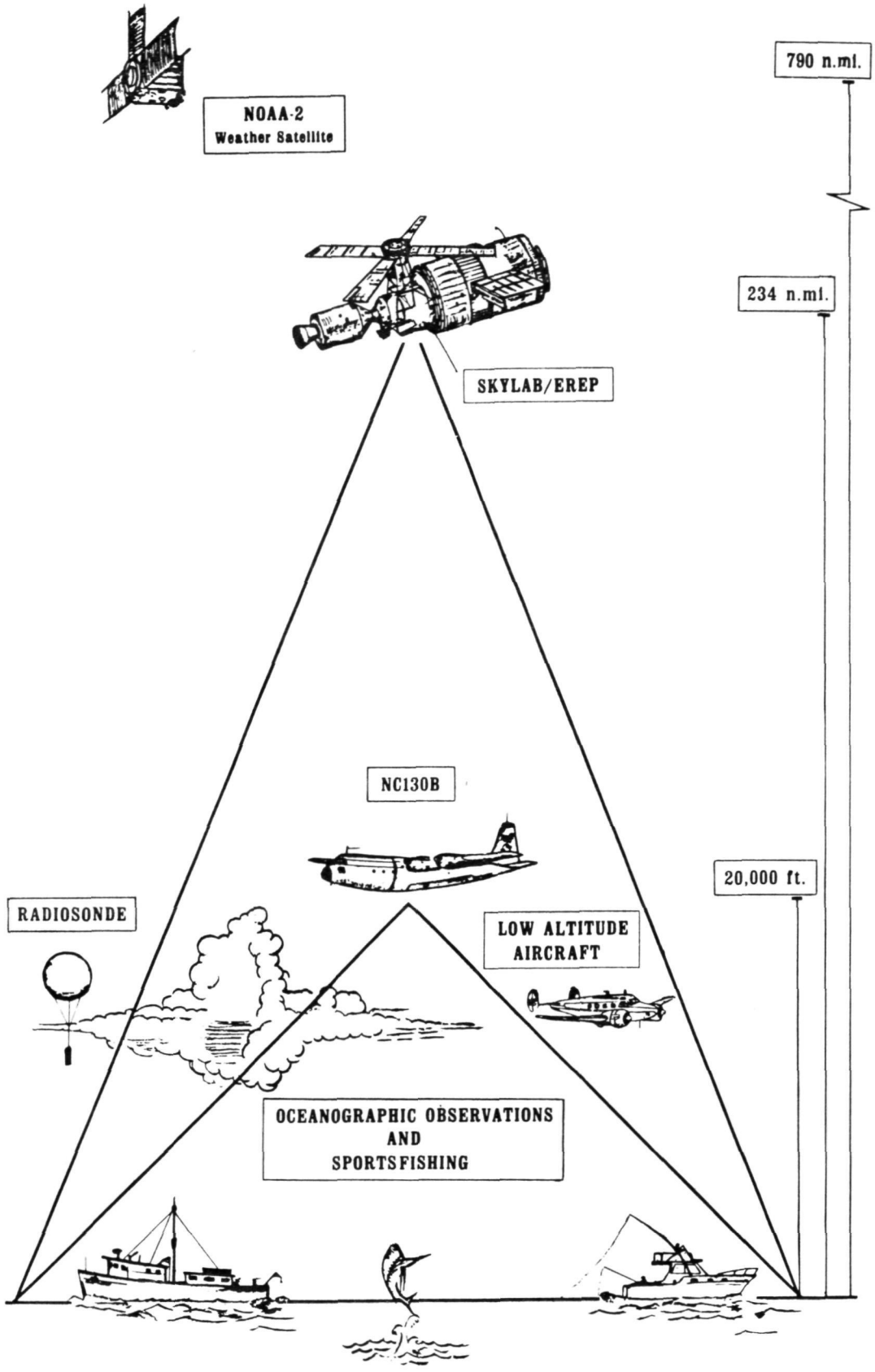

Figure 2. Operational Overview

TABLE I. SKYLAB EREP SENSORS ACTIVATED

INSTRUMENT	DESCRIPTION	FOOTPRINT	APPLICATION
S190 A	6 Cameras	163 km. wide	Water Color, Surface Features
S190 B	1 Camera	109 km. wide	Water Color, Surface Features
S191	Infrared Spectrometer	.43 km. wide	Water Color, Sea Surface Temperature
S192	Multispectral Scanner	74 km. wide	Water Color, Sea Surface Temperature
S194	Microwave Radiometer	109 km. wide (half power)	Sea Surface Salinity

TABLE II. AIRCRAFT SENSOR COVERAGE

INSTRUMENT	DESCRIPTION	FOOTPRINT	USE
NASA NC130B			
MSS	Multispectral Scanner	10.2 km	Sea Surface Temperature, Water Color
RECON IV	Infrared Scanner	7.0 km	Sea Surface Temperature
AMPS	Airborne Multispectral Photographic System	2.3 km	Water Color
RC8	Aerial Camera/Color Photography	9.1 km	Cloud Cover, Water Color, Location of Surface Vessels and Features
I^2S	Multiband Camera	5.3 km	Water Color
PRT 5	Precision Radiation	0.2 km	Water Color
NASA Light Aircraft			
RS-18	Thermal Infrared Scanner	7.3 km	Sea Surface Temperature
K-17	Aerial Camera/Color Photography	4.8 km	Water Color, Surface Features
EL 500	2 Cameras - Color and Color IR	4.2 km	Water Color, Surface Features
PRT 5	Precision Radiation Thermometer	0.1 km	Sea Surface Temperature
E 20-D	Spectrometer	0.1 km	Water Color

Fishing tournament officials restricted competition for trophies to seven offshore gamefish species.

Blue Marlin, Makaira nigricans
White Marlin, Tetrapturus albidus
Sailfish, Istiophorus platypterus
Wahoo, Acanthocybium solanderi
Dolphin, Coryphaena hippurus
Yellowfin Tuna, Thunnus albacares
Bluefin Tuna, Thunnus thynnus

Approximately 325 anglers fished from craft, 20 to 57 feet in length, scattered over the test area. On each boat a gamefish log was kept of all fish raised, hooked, lost and boated. Gamefish samplers collected the logs in the late afternoon at the checkpoints from the returning boats. At the time of submission, each log was reviewed by a gamefish sampler with the respective boat captain for omissions and errors while details still remained fresh in mind. Table III gives a breakdown of the fish catch.

Sea Truth Measurements

Data task teams on four Government and five Government-chartered vessels operating out of Orange Beach, Alabama; Destin, Florida; and Panama City, Florida, gathered sea truth environmental data at 48 sampling stations at periodic intervals during daylight hours on August 4 and 5. A total of 140 sets of measurements were taken.

TABLE III. TOURNAMENT FISH CATCH

Fish Species	No. Raised But Not Hooked		No. Hooked		No. Lost		No. Boated	
	4 Aug.	5 Aug.	4 Aug.	5 Aug.	4 Aug.	5 Aug.	4 Aug.	5 Aug.
	BILLFISH							
Blue Marlin	5	3	6	5	6	5	0	0
White Marlin	25	19	32	23	9	14	23	9
Sailfish	4	5	10	4	6	3	4	1
Total Each Day	34	27	48	32	21	22	27	10
	OTHER GAMEFISH							
Yellowfin Tuna	0	0	0	0	0	0	0	0
Bluefin Tuna	0	0	0	0	0	0	0	0
Dolphin	2	0	32	43	5	5	27	38
Wahoo	4	0	10	6	2	3	8	3
Total Each Day	6	0	42	49	7	8	35	41
	ALL TOURNAMENT GAMEFISH							
Total Each Day	40	27	90	81	28	30	62	51
Tournament Totals	67		171		58		113	

Parameters measured for each set included surface water temperature, air temperature, Secchi disc extinction depth (as a measure of turbidity), sea state, wind direction and speed, wet and dry bulb temperature, water depth, atmospheric pressure, visibility, cloud cover and type, and water color. Sea water samples were also taken for laboratory analysis for salinity and chlorophyll-a, -b, and -c. The Forel-Ule color comparator was used to determine water color. Sea surface temperature was obtained by means of a bucket thermometer. In addition, portable salinometers were used on several vessels to obtain in situ salinity and temperature measurements.

In addition to data acquisition by the oceanographic vessels, scientific observers on twelve of the larger gamefishing boats collected sea truth data coincident with gamefish catches. A total of 75 sets of measurements were taken by these observers. Parameters measured were the same as those measured from the oceanographic boats except that chlorophyll samples were not taken. Psychrometer readings were taken on only a few boats.

DATA ANALYSIS

Approach

The sensors used in this investigation did not have the capability for direct observation of gamefish and had only limited capability for acquisition of information related to surface or near-surface phenomena. Therefore, the main thrust of the data analysis utilized an indirect approach with intermediate correlations. The resource data and remotely sensed information were separately related to the sea environment as observed by surface sampling and related through the sea environment to each other (Figure 3). An effort to relate surface phenomena directly with the incidence of gamefish was unavailing.

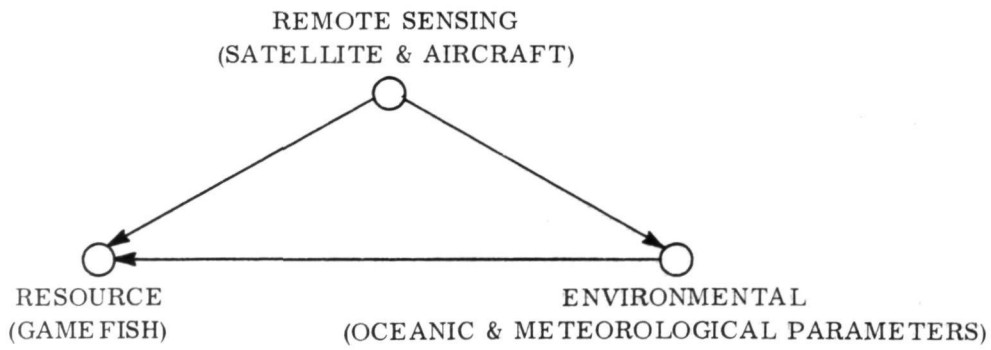

Figure 3. Analysis Approach

The objective of the analysis was to produce a prediction model, using oceanographic values inferred from remotely sensed data, which could be used as a management tool for resource utilization.

RESOURCE AND SEA TRUTH RELATIONSHIPS

Concept

The concept employed in the analysis was that oceanic gamefish abundance and distribution can be expressed as a function of the environment, which is similar to that concept expressed in a

previous fisheries remote sensing paper (5). The functional dependence is described in the following algebraic expressions.

$$A_{x,y} = f(E)$$

$$D_{x,y} = g(E)$$

where:

A = number of oceanic gamefish
x,y = fish location coordinates
E = environmental conditions at x,y
D = gamefish distribution parameters

$$D = \begin{cases} 0 & \text{no fish present} \\ 1 & \text{fish present} \end{cases}$$

The abundance parameter, $A_{x,y}$, was estimated by oceanic gamefish raised only, hooked, lost, or boated by the fishermen and therefore has a larger degree of error due to the ability of anglers to identify, attract, hook and land the fish. The distribution parameter, $D_{x,y}$, by its definition was less susceptible to error than the abundance parameter, $A_{x,y}$, and therefore was utilized in the mathematical modeling efforts.

Data Preparation

Resource information was available for only 34 out of the 54 fishing squares on 4 August and 30 out of the 54 squares on 5 August. However, environmental information was not obtained from some squares for which there were catch data. Accordingly, an averaging technique was used to provide environmental information for those squares where resource data had been recorded. The technique consisted of averaging the values of all encircling squares and has previously been used for interpolating catch data (6). Furthermore, individual test square values for each parameter were computed by averaging all station readings in that square for that parameter each day. Environmental data for each square fished consisted of the following parameters: surface water temperature, surface salinity, air temperature, Secchi extinction depth, sea state, Forel-Ule water color, chlorophyll-a, chlorophyll-b, chlorophyll-c, water depth, and distance from shore. These parameters were utilized as independent variables in the initial correlation analyses. Atmospheric pressure was eliminated from the analyses because of the limited number of stations for which this measurement was reported.

It was decided to concentrate efforts on a billfish and a non-billfish species. White marlin and dolphin respectively were selected for study because a relatively large catch data set was available for each. The white marlin was selected initially because interest seemed to focus on billfish and accordingly, much of the text on the progress of the analyses relates to white marlin.

Initial correlation analyses were made to determine which form of the resource abundance and distribution parameters (fish raised only, hooked, raised plus hooked, or boated) should be used. The hooked parameter was found to have the strongest correlation with the environmental parameters. This stronger correlation can be explained by less error in this measurement as compared to the raised parameter, i.e., there is less chance of incorrect identification once the fish is hooked. Conversely, the boated parameter, which had no possibility of identification error, caused a significant error in the distribution parameter, $D_{x,y}$, when the fish was hooked and not boated.

Therefore, the hooked form of the parameter was used in correlation analyses and mathematical modeling.

Further error was identified in the resource distribution parameter in that a certain level of fishing pressure was required to determine if there were fish in a fishing square. In other words, if fishing pressure was insufficient in a given square, the distribution parameter would have a value of 0 regardless of the presence or absence of fish. This would tend to conceal relationships between the resource and the environment. Having found that no white marlin were caught in any of the test squares with less than 4 boat hours of fishing pressure, a correction for this error was made by eliminating from the analyses all squares having less than 4 boat hours of fishing pressure. This resulted in narrowing the study to 24 out of the 34 test squares remaining for 4 August, and 22 out of the 30 remaining for 5 August.

Correlation Analysis

Correlation and regression techniques were utilized to define relationships between the resource and the environment as defined by sea truth measurements. The number of white marlin hooked in each test square was utilized as a measure of abundance ($A_{x,y}$) and converted to form the distribution parameter ($D_{x,y}$). Linear correlation coefficients were computed for white marlin abundance and distribution and each of the environmental parameters (Table IV) measured on 4-5 August. The results listed in Table IV show a difference between abundance and distribution and probably reflect error in the abundance parameter. The dubious quality of the abundance parameter led to emphasis on the distribution parameter in the modeling efforts. It should be stressed here that the correlation coefficients are a measure of the linear relationships between the given dependent variables and each environmental parameter respectively, and do not necessarily indicate the set of parameters which should be used in developing predictive models. This is due to the fact that in some cases the parameters listed are also statistically correlated. For example, in the test area, water depth and distance from shore have a correlation coefficient of .832 which is significant at the 99% level. Hence, these two parameters are not statistically independent and one or possibly both (depending on interrelation with other parameters) may not be selected as a model parameter. However, the correlation coefficients listed in Table IV provide a measure of the linear relationship (within this set of data) between the white marlin parameters and each of the environmental parameters.

Assignment of biological significance to these correlations was not within the scope of this study. The parameters measured may only be serving as indices of unmeasured parameters. Other investigators (7) have also found temperature to be related to fish distribution. In analyses of the distribution of white marlin Gibbs (7) found that successful white marlin longline sets were made in surface water temperatures above 24°C. Since the fishing data were collected in August when the Gulf is nearly uniform in surface temperature, 29°C (8), the large catch of white marlin was not unexpected. A factor which should be noted here is that there was a correlation coefficient of .407 significant at the 99% level for white marlin distribution and temperature with all of the sampled temperatures measuring between 28.5°C and 31.6°C. The strong positive correlation held true for data taken on both days as well as the combined data sets.

There is no evidence of correlation of either distribution or abundance with depth of water according to Gibbs (7). Thus, the apparent strong depth correlation listed in Table IV may be valid only in this particular test area and may be seasonal or coincidental.

Positive correlations (significant at the 90% level) between white marlin distribution and the chlorophyll-a and c (phytoplankton measurements) were found. This may be compared to a white marlin study in the Middle Atlantic Bight where important marlin areas showed distinctly high zoo-

TABLE IV. CORRELATIONS BETWEEN WHITE MARLIN (HOOKED) ABUNDANCE ($A_{x,y}$) AND DISTRIBUTION ($D_{x,y}$) ESTIMATES AND SAMPLED ENVIRONMENTAL PARAMETERS (E)

Parameter	Degrees of Freedom	Correlation Coefficient (r)	
		Distribution	Abundance
Water Temperature (°C)	44	.407***	.310**
Salinity (ppt)	44	-.145	.001
Air Temperature (°C)	44	.113	.218*
Secchi Transparency (m)	44	.129	.269**
Sea State (m)	44	.272**	.183
Forel-Ule Color (units)	44	-.180	-.044
Chlorophyll-a (mg/m^3)	44	.200*	.054
Chlorophyll-b (mg/m^3)	44	.056	-.005
Chlorophyll-c (mg/m^3)	44	.214*	.241*
Water Depth (m)	44	.329**	.170
Distance from Shore (km)	44	.454***	.323**

* 90% significance level ** 95% significance level *** 99% significance level

plankton volumes (9). The comparison tends to support the correlation if one assumes that zooplankton abundance is a function of phytoplankton abundance.

As planned, subsequent to the white marlin analysis, correlations were investigated for 4 and 5 August and the combined dates between dolphin distribution and abundance and the environmental parameters - sea surface temperature, salinity, air temperature, Secchi extinction depth, sea state, Forel-Ule color, water density and chlorophyll-a, -b, and c. Instability was found to exist for all relationships on a day to day comparison. The extent of the instability discouraged development and testing of prediction distribution and abundance models for dolphin such as were accomplished for white marlin.

REMOTELY SENSED OCEANOGRAPHIC PARAMETERS AND CORRELATIONS WITH THE ENVIRONMENT

The object of this phase of the experiment was to measure water surface temperature, turbidity, and chlorophyll concentration from aircraft and satellite. Techniques currently under development

by the NASA ERL were used for the measurements.

Sea Surface Temperature

The remote measurement of sea surface temperature has been widely studied. Absolute accuracies of 0.5°C are readily obtainable from aircraft measurements using one, or in some cases no ground truth calibration (10) (11) (12) (13).

The aircraft thermal data were taken from 3000 meters with an RS-18 scanning radiometer and a PRT-5 radiometer and also from 6100 meters with another PRT-5 radiometer. These radiometers are sensitive in the 8-14 μm regions of the spectrum. The aircraft thermal data have been processed and a radiometric temperature trace along the flight lines developed (Figure 4). From this trace, the temperature at points between the flight lines was interpolated to provide the basis of the contour map shown in Figure 5. For comparison purposes, the contour map of surface temperature determined by surface measurements and corrected for insolation during the ten-hour period of sampling to a time midway through the remote data acquisition exercise is presented in Figure 6. The time correction was performed by computing the change in temperature averaged over the test area on an hourly basis and adding the appropriate change to readings made at times different from the normalization time. A composite of the thermal data from the two aircraft was made to fill in gaps that occurred at different locations along the flight lines for the two aircraft caused by time-varying cloud cover. There were, however, several locations along the flight lines where clouds caused a total loss of data, and other locations where anomalous temperature measurements may have resulted from severe variations of atmospheric conditions.

Comparison of the surface and remote temperature contour maps shows that, while they are not identical, the same basic trends are present in both maps. There are two likely explanations for the discrepancies. The surface measurements were made by many individuals under different conditions, which could easily result in measurement errors of up to 0.2°C (14). Because of the 0.25°C contour interval, errors of this magnitude would distort the contour patterns. A second explanation is the heterogeneous atmosphere perturbing the remotely measured surface temperature. Analysis of general atmospheric conditions over the test area shows that a variation of 0.23°C can be expected excluding local anomalies due to cloud formations.

It was anticipated that Skylab S192 data would provide thermal measurements over the entire test area. However, analysis of the S192 thermal data has been delayed until June 1975.

Chlorophyll

Measurement of chlorophyll-a concentration obtained from radiance measurements has been attempted with varying degrees of success by many workers (15) (16) (17). No technique has apparently achieved either sufficient accuracy or consistency to be generally accepted as the best remote measurement method. The remote data processed in the study thus far were obtained by an Exotech 20-D spectral radiometer, flown on the light aircraft at 3000 meters. The instrument, as configured for this experiment, measured radiance in the region of the spectrum from 390 to 1100 nanometers (nm) and calibrated at 57 wavelengths in that range.

An algorithm for computing chlorophyll-a concentration developed by Weldon (15) has been used successfully with data taken with this radiometer, but at lower altitudes over the Mississippi Sound. Weldon's technique consists of a linear function of the difference between the radiance at 620 and 470 nm, normalized by the radiance at 520 nm. The coefficients of the function are determined

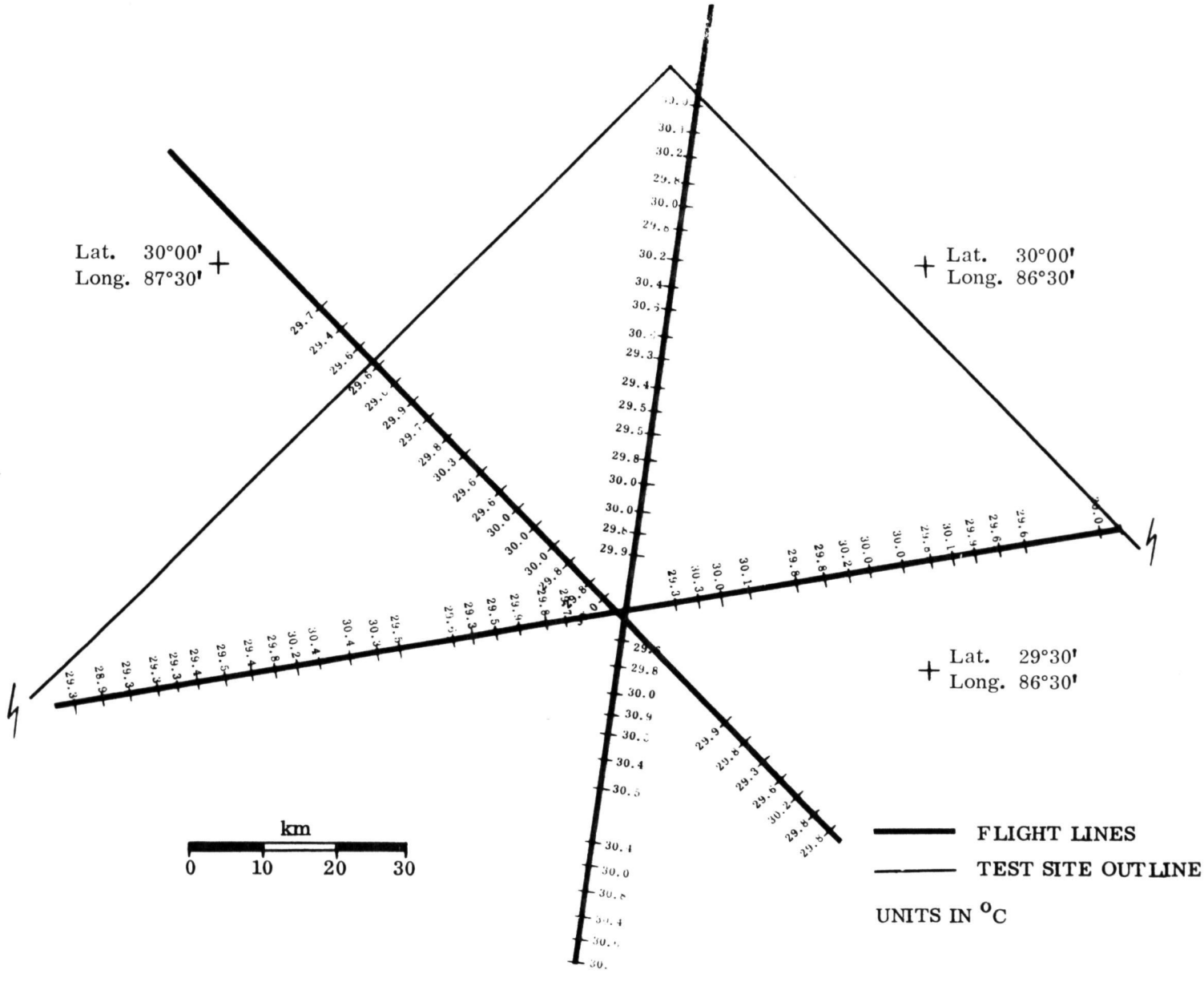

Figure 4. Radiometer Temperature Trace Along Flight Lines

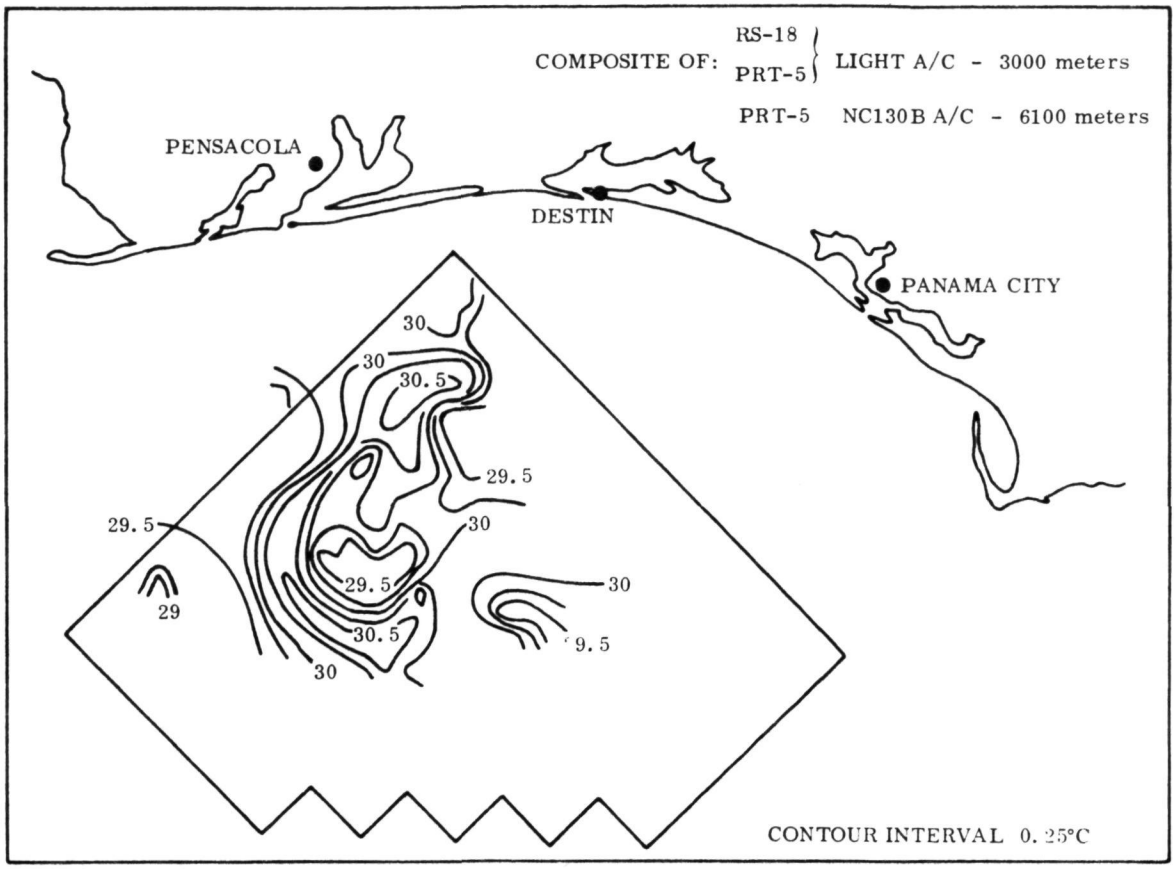

Figure 5. Remote Measurement of Water Temperature

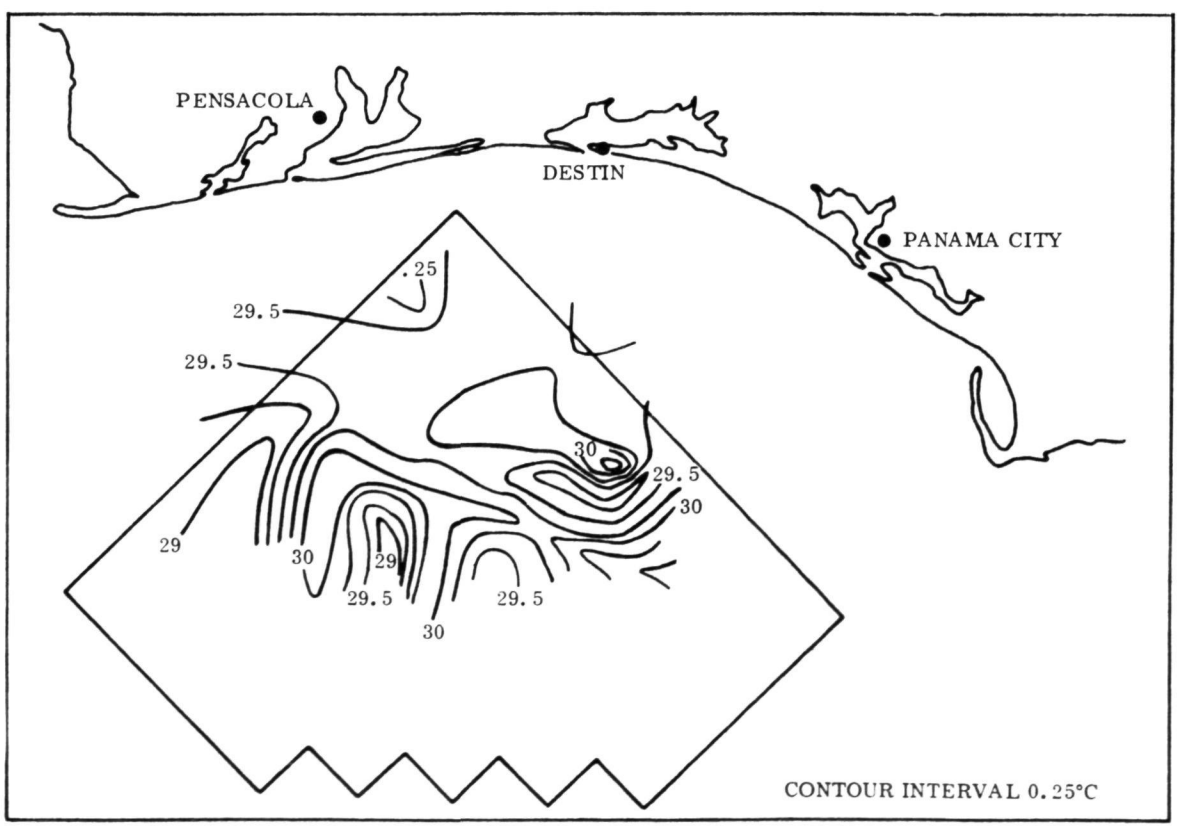

Figure 6. Surface Measurement of Water Temperature

from ground truth data.

$$C_W = \alpha_1 (R_{620} - R_{470}) / R_{520} + \alpha_2 \qquad (a)$$

This algorithm was applied to the data acquired in this experiment. The root mean square (rms) deviation of these calculations from the surface measurements was 0.48 mg/m^3 for 18 measurement points, of which nine were used for calibration.

Another technique was used for computing chlorophyll-a concentrations. Examination of the correlation of the 520 nm normalized radiance at each of the 57 wavelengths indicated that the chlorophyll-a concentration was highly correlated with the radiance at 470 and 600 nm. Further analysis showed that a linear combination of these radiance values correlated very well with the square of the chlorophyll-a concentration, so a second calculation of the chlorophyll-a concentration based on spectral radiometer measurements was made using the relation shown in Equation (b).

$$C_c = \sqrt{\alpha_1 (R_{600} - R_{470})/R_{520} + \alpha_2} \qquad (b)$$

Figures 7 and 8 are the contour maps drawn from the surface and remote measurements of chlorophyll-a, respectively. The remote measurements are a composite (Figure 9) of the results of both calculations. Careful examination of the two sets of measurements showed that the second gave better results in areas where chlorophyll-a content was low (0.28 mg/m^3 rms error), but that the response flattened out at concentrations above 2.3 mg/m^3. The first technique was better at the higher concentrations, so when a concentration greater than 2.0 mg/m^3 was indicated by the second technique, the value predicted by the first technique was used; otherwise, the value was that computed from Equation (b). The rms deviation of the composite at the 18 surface comparison points was 0.44 mg/m^3.

Comparison of Figures 7 and 8 shows that, while the maps do show significant differences, the large variations present in the surface data are also found in the remote data. This may be readily observed in Figure 10 which is a comparison of chlorophyll-a remote and surface measurement profiles along flight line two. In addition, there are some rapid changes indicated in the remote data which are not seen in the surface data. This does not mean that either measurement is in error; the remote data is a continuous sampling while the surface measurements are separated by approximately an hour's cruise. Another factor to be considered is the 10% repeatability factor (18) of the surface chlorophyll-a determination. It must also be remembered that no corrections for atmospheric conditions were made. These conditions were not constant over the test area, and clouds and cloud shadows do affect the apparent color and hence the inferred chlorophyll-a content.

Turbidity

For this experiment, turbidity was measured as Secchi extinction depth. This surface truth measurement of turbidity was used because of operational considerations, i.e., the technique is simple and the necessary equipment inexpensive. However, the measurement is subjective because of the human factor involved and is thus susceptible to considerable error.

Weldon (15) developed an algorithm for computing Secchi extinction depth from spectral radiometer measurements, so the first attempted remote measurement of turbidity was with this technique. Weldon (15) found that the Secchi extinction depth was proportional to the ratio of the radiance measured at 600 nm to that at 550 nm, but application of this algorithm to the data acquired in

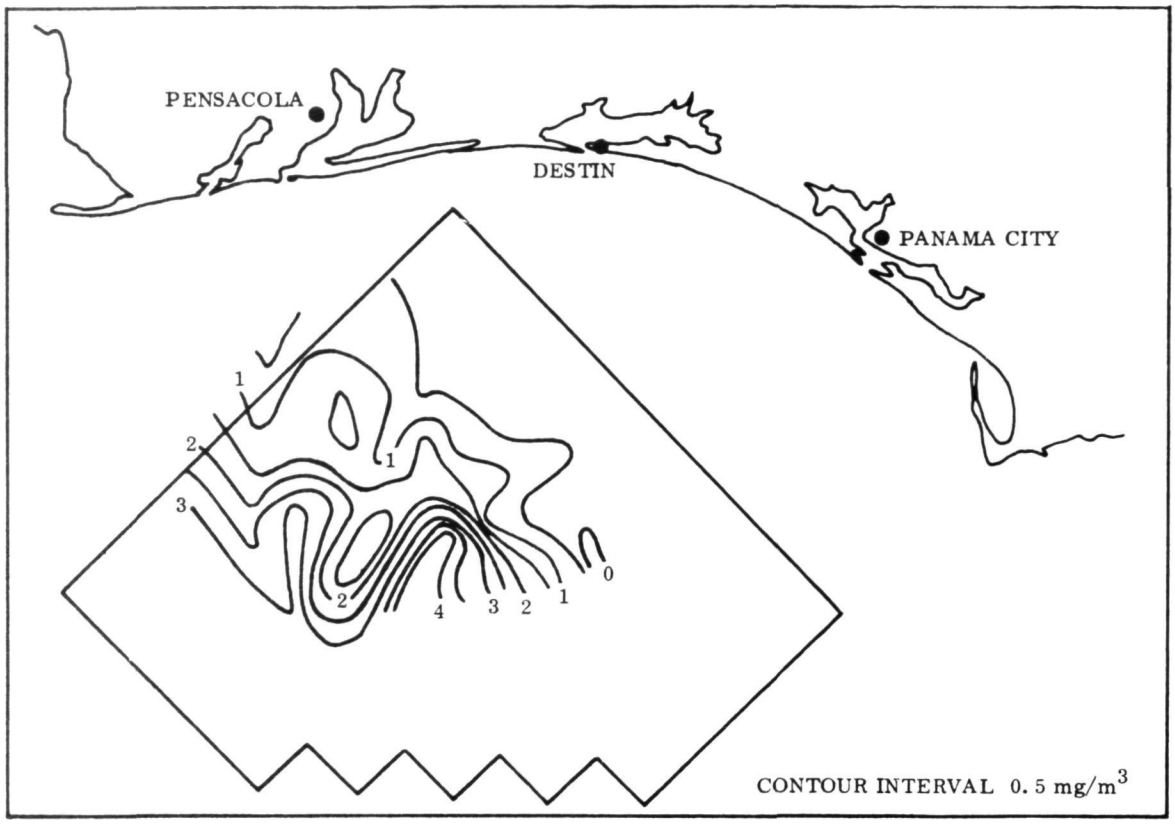

Figure 7. Surface Measurement of Chlorophyll-a

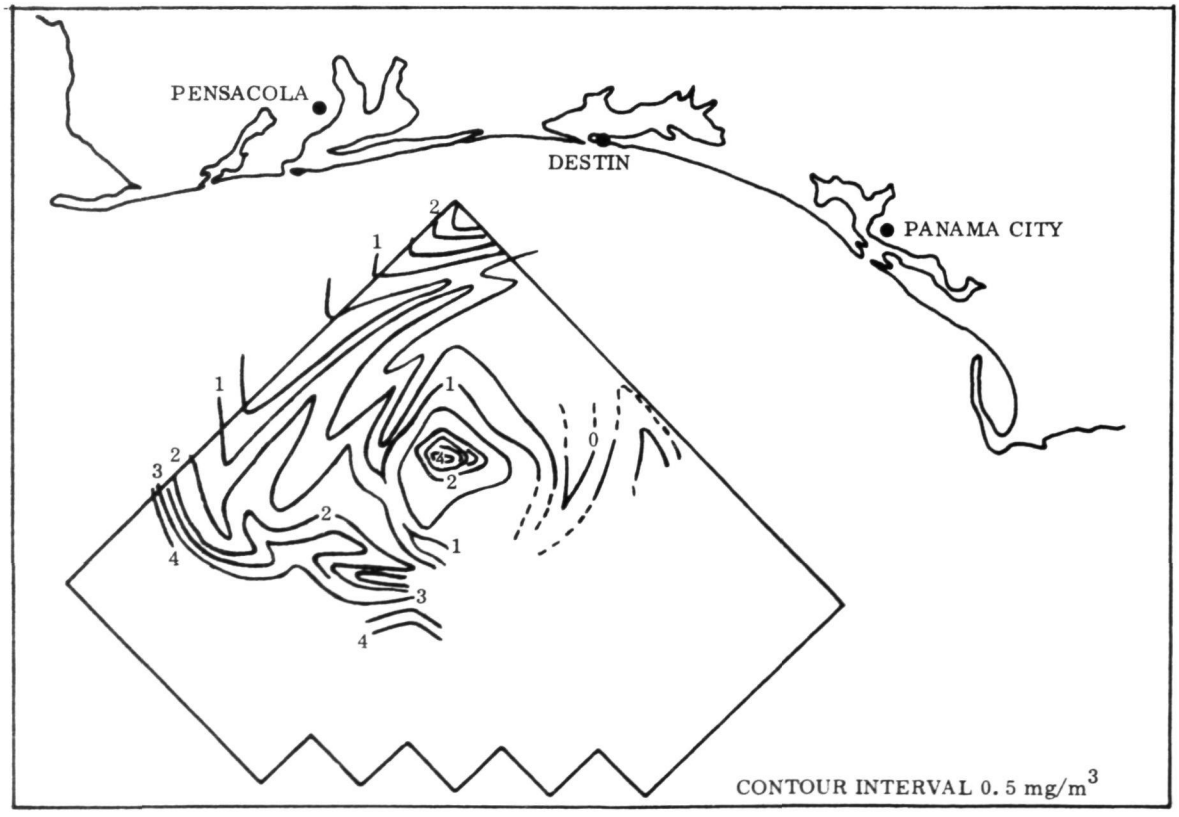

Figure 8. Remote Measurement of Chlorophyll-a

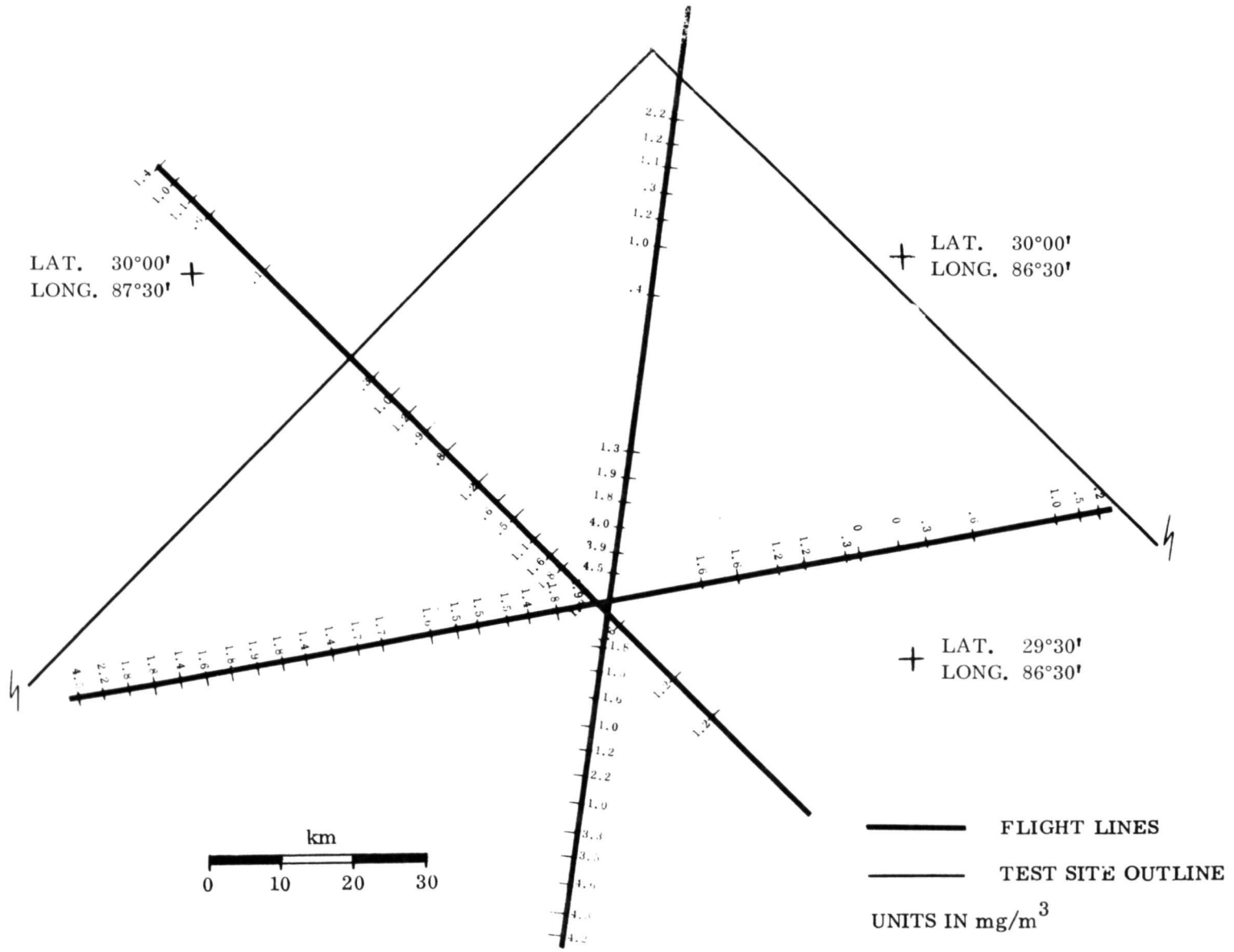

Figure 9. Chlorophyll-a Along Flight Lines

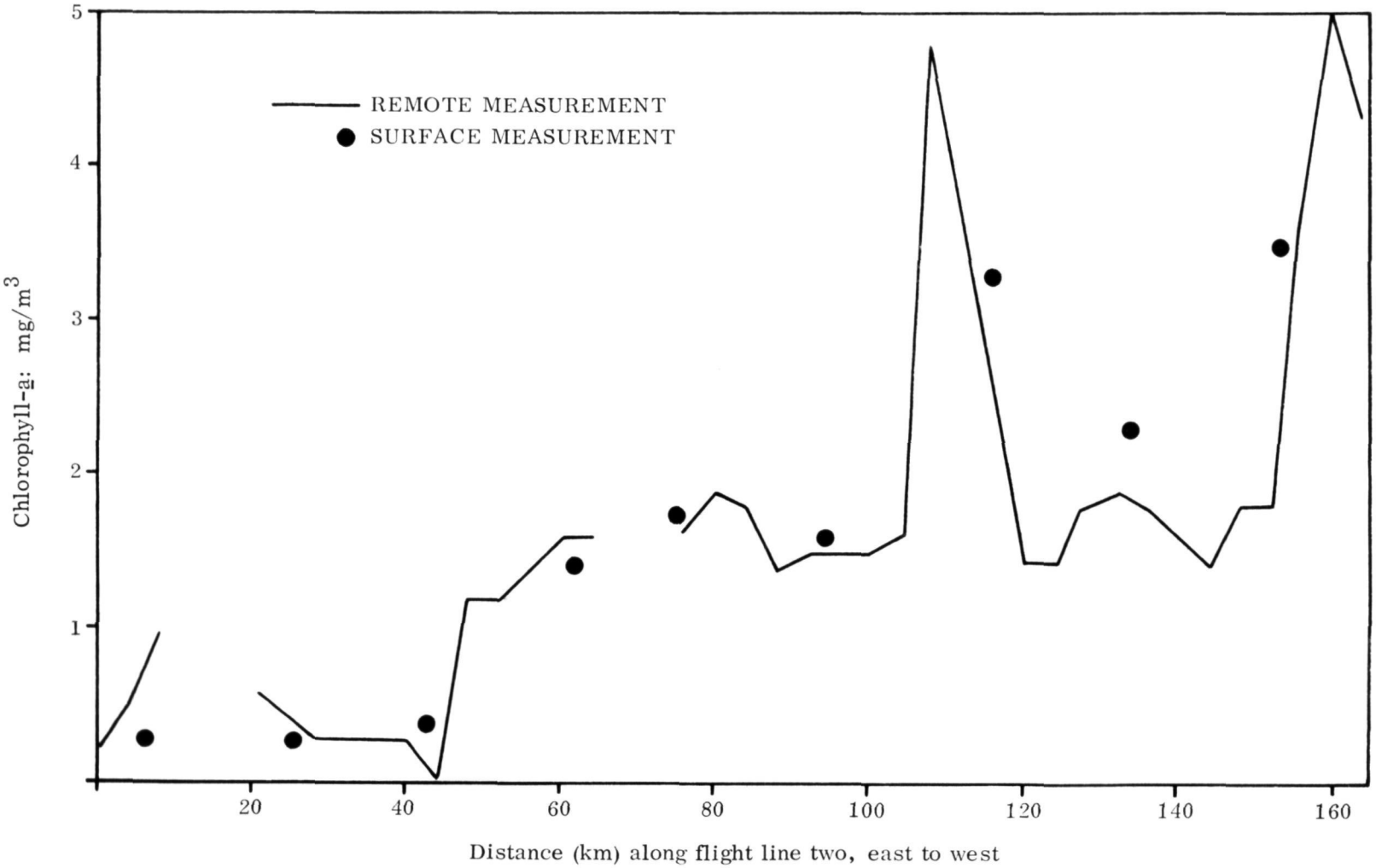

Figure 10. Comparison of Chlorophyll-a Remote and Surface Measurement Profiles Along Flight Line Two

the gamefish experiment was notably unsuccessful. The failure of this previously verified technique is probably due to the fact that Weldon's work was done with measurements made in the Mississippi Sound where three meters is generally the greatest Secchi depth observed, as opposed to thirty in the Gulf. Several techniques were developed to infer turbidity measurements from the spectrometer data.

The final algorithm as in the chlorophyll calculation optimized the information content relative to the Secchi transparency measurement. This optimization was performed by selecting wavelengths which showed the highest correlation with the Secchi depth and the least correlation with each other. Unnormalized radiance data, radiance normalized by a wide band in the blue (390-430 nm) region, and radiance normalized by a wide band in the infrared (911-1073 nm) region were examined. The best set of correlations was found with three wavelengths (410, 440, and 550 nm) of the blue-normalized radinace. An expression of the form

$$S_c = \sum_{n=1}^{3} \alpha_n R\lambda_n / R_{blue} + \alpha_4 \qquad (c)$$

was used to calculate the Secchi extinction depth.

The results are in agreement with the surface measurements as can be seen from Figures 11 and 12 which are contour maps of the Secchi extinction depth made from surface and remote measurements according to this technique. While the calculated rms error was 3.9 meters for 20 points, of which eight were used for calibration, the trends were well represented. The chief discrepancy between the two is in the area where surface readings on the order of 30 meters were made and where the remote measurement indicates greater turbidity.

There are two likely explanations for this variation. Because of the criteria used in selecting calibration points for the remote measurements, which included a maximum time difference between surface and remote measurements of three hours, no calibration points had Secchi depths of more than 17 meters. This would introduce an uncertainty of unknown magnitude into measurements outside the calibrated range. Also, reports from the surface observers indicated that water conditions were changing over the test area. It is thus possible that the sea conditions changed at this sample station during the four hour interval separating surface and remote measurements.

Salinity

Because salinity is an important factor in the white marlin predictor to be described later, it would have been desirable to use remote measurements of salinity in this experiment. The feasibility of applying L-band radiometer data to measure salinity remotely has been demonstrated by Thomann (19). Unfortunately, the microwave radiometer necessary for this measurement was not available for use on the aircraft for this experiment; the other potential source for remote salinity measurements was the L-band radiometer on Skylab. Unfortunately the footprint of the instrument was almost as large in area as the entire test site, resulting in insufficient resolution.

RESOURCE AND REMOTELY SENSED DATA RELATIONSHIPS

Approach

Fishermen in search of gamefish consider, as a rule, the color of the sea as the primary indicator of good fishing grounds. The generally accepted theory is that the gamefish are found principally

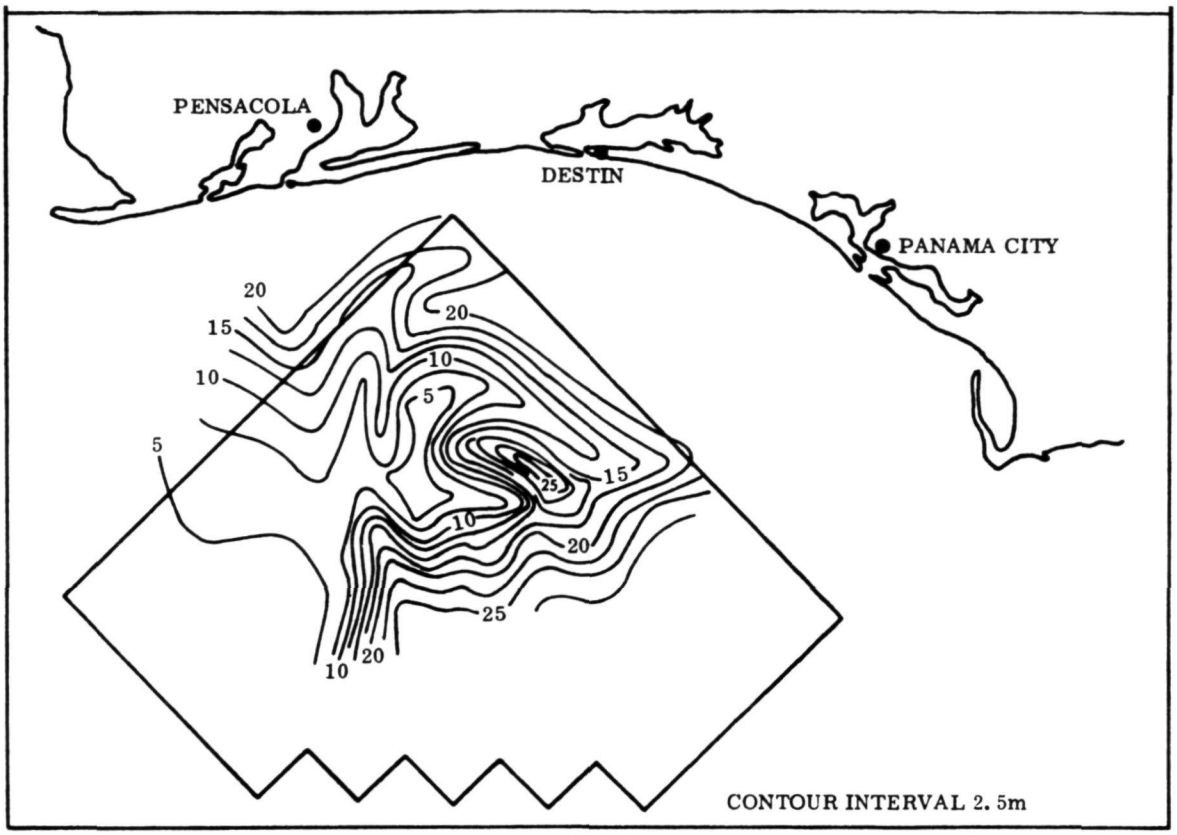

Figure 11. Surface Measurement of Turbidity (Secchi Extinction)

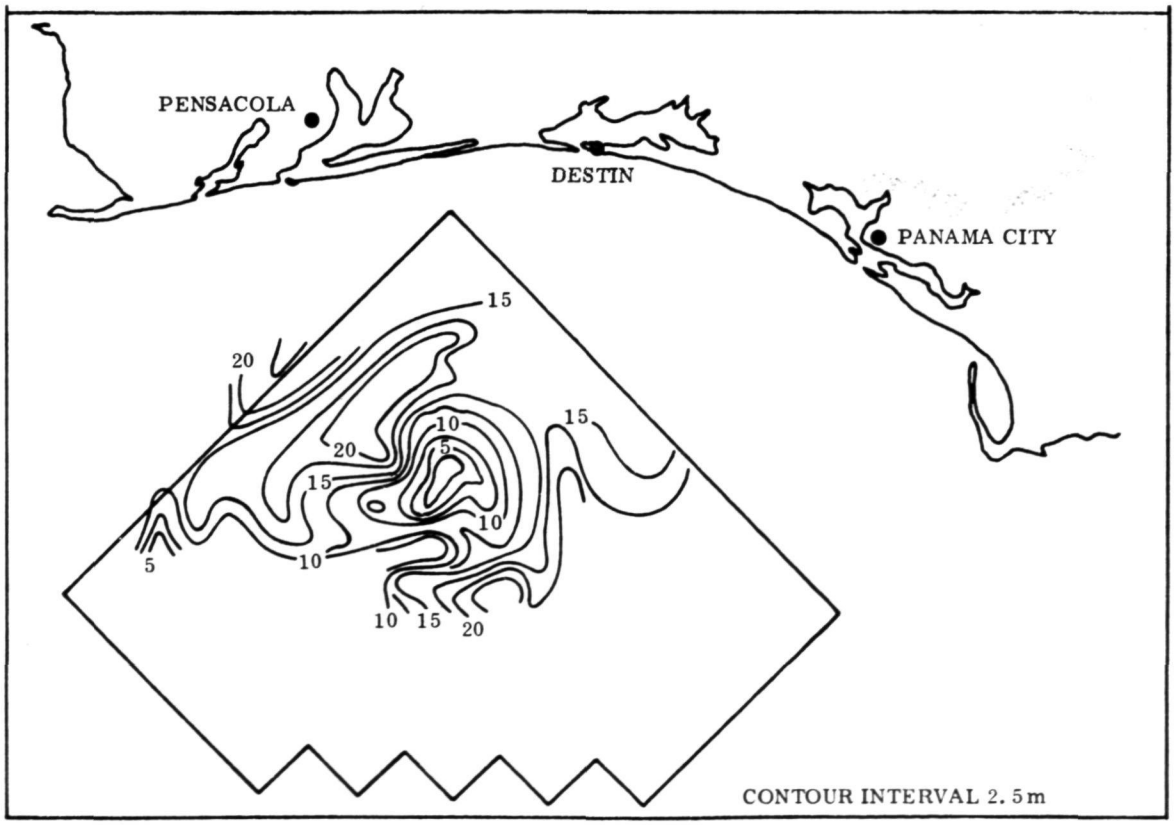

Figure 12. Remote Measurement of Turbidity

in areas where the water is blue as opposed to green. The approach taken in attempting to define a relationship between the billfish resource and marine phenomena directly sensible by the satellite and aircraft sensors utilized visual interpretation, color enhancement of multiband photography, and direct correlation between spectral radiometer "color" measurements and resource distribution information.

Water Discontinuities

The photography from the NC-130B and the light aircraft were visually examined for surface discontinuities which would indicate the boundary between different water masses. The discontinuities searched for were either sharp changes in water color, of which none were found, or surface rips. Many rips were identified, some in both sets of aerial photography. Unfortunately, the portion of the test site visible in the photography was small, therefore much of the study area could not be included in this analysis of the aerial photography.

Figure 13 shows the relationship between rips and white marlin hooked. The fishing squares containing rips are indicated by horizontal lines. Squares where fish were hooked are shaded. The limited data set does not permit any definitive conclusions to be drawn concerning fish/rip relationships, but one must observe that there are no fish caught in squares containing rips.

No rips were found in the Skylab S190A or S190B photography which has been examined in detail. This is to be expected since these surface features generally have widths less than the resolution of both the S190A and S190B sensors.

S190A Photographic System

The S190A multispectral photographic system consisted of six high-precision cameras with matched optical systems. Each had an F/2.8 lens with aperture variable to F/16 in 1/2-stop increments and a focal length of 15.2 centimeters (6 inches). At a nominal spacecraft altitude of 435 kilometers (235 nautical miles), the 21.2-degree square field of view provided ground coverage 163 kilometers (88 nautical miles)square. The film width was 70 millimeters, which provided a usable image 5.7 centimeters (2 1/4 inches)square. The camera system compensated for the forward motion of the spacecraft along the flight path. Each of the six cameras was identified by a station number and equipped with combinations of filters and films for the various wavelength bands (Table V).

Positive black and white transparencies of the experimental area for stations 1, 2, 5, and 6 and positive color transparencies for stations 3 and 4, scaled at 1:2,850,000 were received as S190A data products from NASA's Johnson Space Center.

Of the S190A film products acquired and received for analysis, black and white (B&W) 70 mm negative transparencies of successive frames 242 and 243 (11:41:04.3 CDT) of all six stations were made and used in density slicing/color enhancement analyses. Neither frame selected would accommodate the entire test area. Figure 14 shows the two frames from station 6 spliced together with the test site overlaid. Pensacola harbor may be seen in the upper right corner. The S190A photograph revealed a number of anomalous dark patches (20) within the sun-glint areas, the largest of which appeared in grid square numbers 31 and 48. This particular patch was oval shaped; it encompassed a total area of about 570 square kilometers and was associated with calm sea state measurements ranging from 30 to 40 cm.

Initially, two bands, 0.5 - 0.6 μm and 0.6 - 0.7 μm were density sliced to derive sea surface

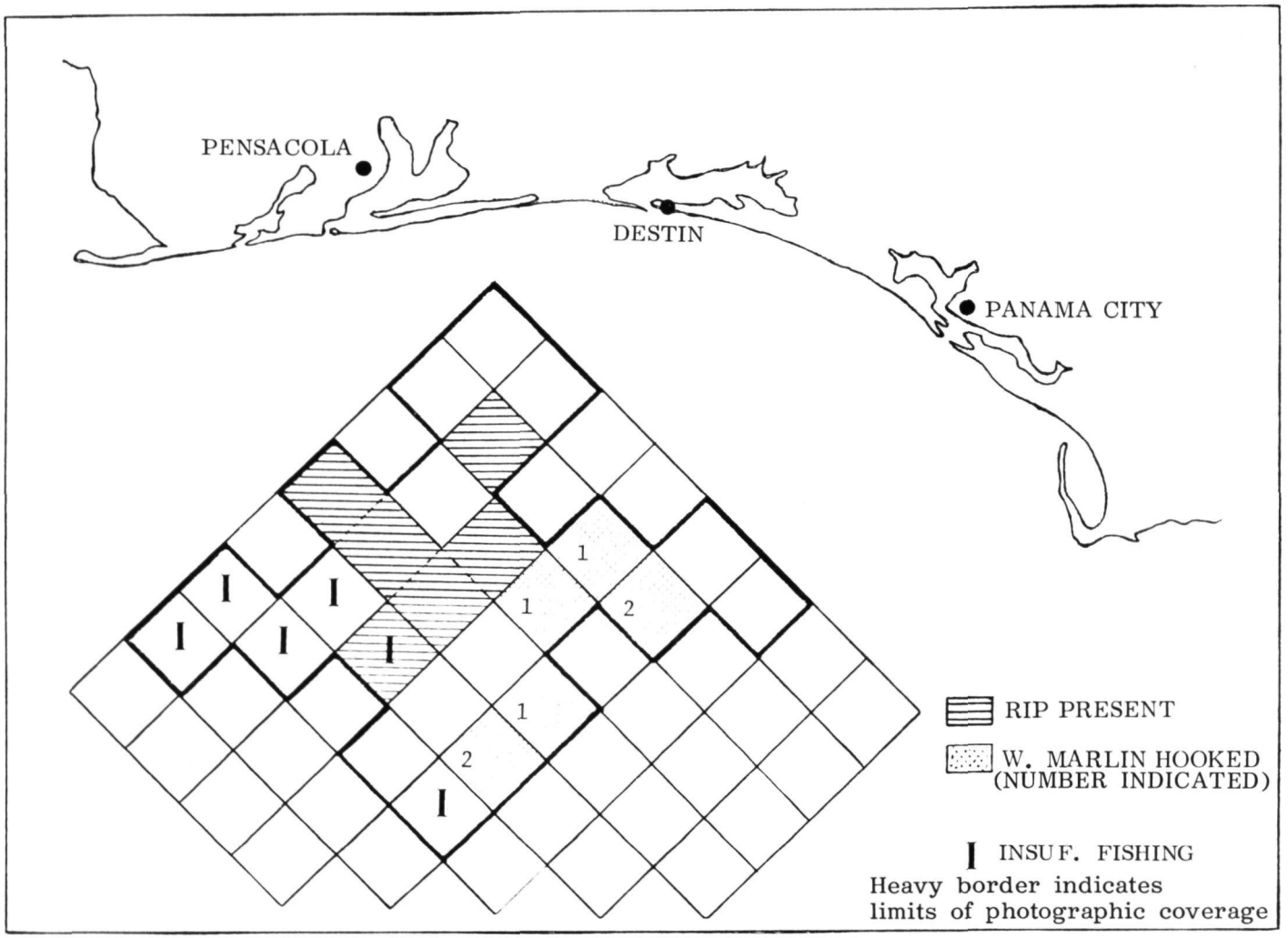

Figure 13. Comparison of White Marlin Distribution with Surface Rip Locations

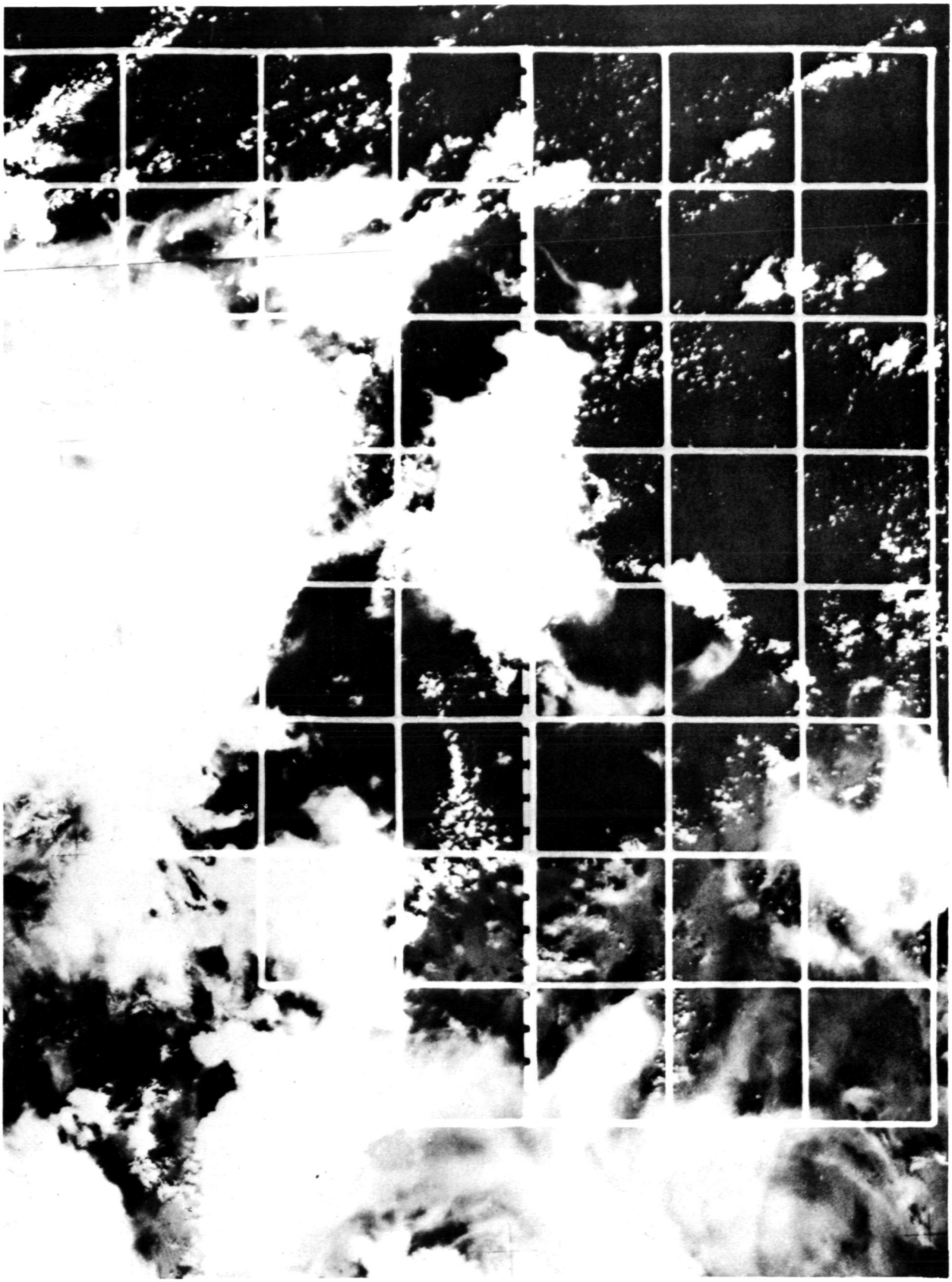

Figure 14. S190A Photography with Test Site and S191 Ground Track Overlay

TABLE V. MULTISPECTRAL CAMERA STATION CHARACTERISTICS

AND FILM ROLLS USED

Sta	Filter	Filter Bandpass, micrometer	Film Type*	Estimated Ground Resolution // meters (feet)	Mission SL-3 Roll No.
1	CC	0.7 - 0.8	EK 2424 (B&W infrared)	73 - 79 (240 - 260)	19
2	DD	0.8 - 0.9	EK 2424 (B&W infrared)	73 - 79 (240 - 260)	20
3	EE	0.5 - 0.88	EK 2443 (color infrared)	73 - 79 (240 - 260)	21
4	FF	0.4 - 0.7	SO-356 (hi-resolution color)	40 - 46 (130 - 150)	22
5	BB	0.6 - 0.7	SO-022 (PANATOMIC-X B&W)	30 - 38 (100 - 125)	23
6	AA	0.5 - 0.6	SO-022 (PANATOMIC-X B&W)	40 - 46 (130 - 150)	24

* Eastman Kodak Company // At low contrast

information. Comparing the distribution of hooked white marlin per square with the image sliced into five density levels revealed that fish were hooked in squares having different density levels. The fishery resource data, as summed and positioned to the center of the squares, therefore could not be correlated with any particular density slice of the S190A multiband Skylab photography as originally anticipated.

Further efforts were made to get by this deficiency by utilizing white marlin catch locations accurately to 1/2 mile (twelve in number) determined by electronic navigation equipment aboard a subset of fishing vessels participating in the experiment. A re-examination of the imagery from stations 1 through 6 was made to determine if the distribution of white marlin was located in a particular density region. The image in Figure 14 was density sliced and color coded on a VP-8 image analyzer. The white marlin locations were superimposed and the resulting image photographed and displayed in Figure 15.

Stations 4 and 6 provided better water detail than the other stations, but as can be seen from Figure 15, no density/white marlin relationship could be established. This does not imply that such a relationship does not exist but only that utilizing this set of fishery data and this set of multiband photography, with band widths previously stated, no relationship could be established. More work is needed in this area of analysis in terms of establishing exact location of the fish, and using S192 data with its narrow-band imaging within the 0.4 to 0.7 µm region and a thermal band as well as digital density slicing and color enhancement techniques to determine if indeed a relationship exists.

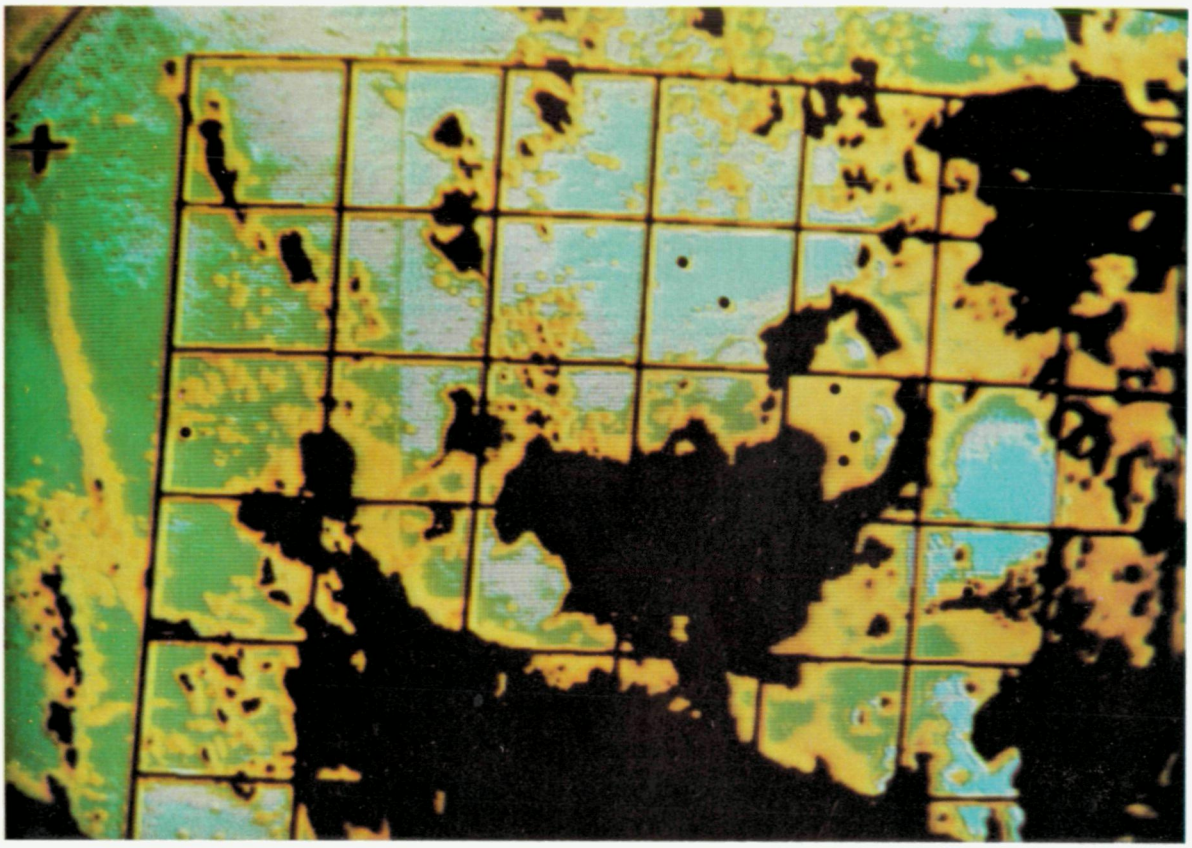

Figure 15. S190A Photography Density Sliced and Color Enhanced with Test Site and White Marlin Locations Superimposed

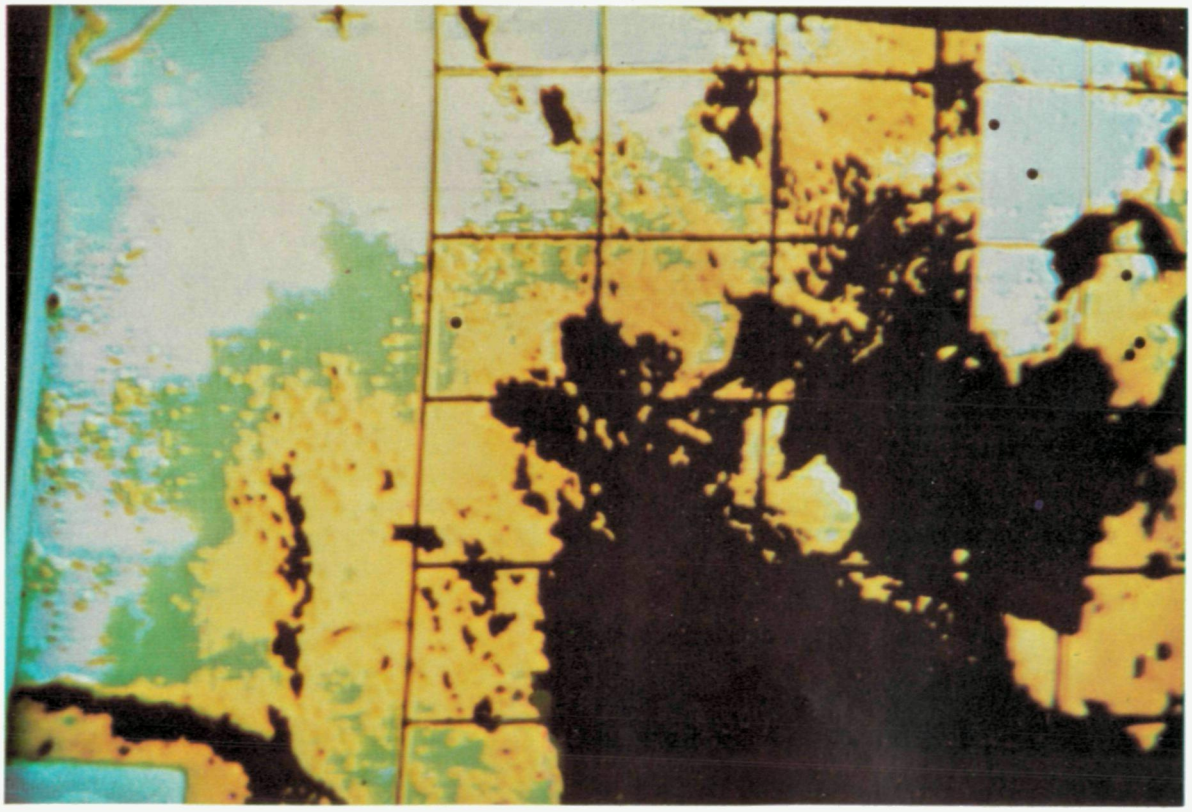

Figure 16. S190B Photograph Density Sliced and Color Enhanced with Test Site and White Marlin Locations Superimposed

S190B Photographic System

The S190B earth terrain camera was a single-lens camera assembly having an F/4 lens with a focal length of 45.7 centimeters (18 inches). The camera system was compensated for Skylab's forward motion and had a field of view of 14.24 degrees which produced a square ground coverage of about 109 kilometers (59 nautical miles). Film width was 12.7 centimeters (5 inches), which provides a usable image 11.4 centimeters (4.5 inches) square. On this particular mission, SO-242 (high resolution color) film was used. The filter bandpass was 0.4 - 0.7 µm and the estimated ground resolution at low contrast was 21 meters (70 feet).

Positive color transparencies of the test area approximately 22.86 x 22.86 cm (9 x 9 inches) scaled approximately 1:500,000 were received as S190B data products from NASA's Johnson Space Center.

Negative black and white transparencies from frames 220 and 221 which were spliced together and reduced to approximately 22.86 x 11.43 cm (9 x 4 1/2 inches).

A transparent overlay, containing the test area and that set of white marlin catch locations which could be located to within one-half mile, was prepared and utilized in the density slicing color enhancement analysis as shown in Figure 16 on the previous page.

The clouds (highest reflected radiance) are colored black and sun-glint areas orange. Sun-glint covers a large area in the lower right hand side of frame 220. Water areas were density sliced into three regions and assigned the colors of green, purple and blue going from highest reflected radiance to lowest reflected radiance. Again no relationship between the density of reflected light in the 0.4 to 0.7 µm range and white marlin distribution could be established from a visual evaluation. Sample size of 8 white marlin locations which could be located to .804 km (1/2 mile) accuracy and fairly clear of cloud cover was somewhat small, therefore no attempt was made to compute statistical correlation between fish location and radiance density values.

One promising aspect of the S190B imagery not a part of this experiment was the fact that several of the sportfishing boats could be seen with the naked eye. The fishing boat shown in Figure 17 is 12.5 meters (38 feet) long and was identified by time/position information taken from fishing logs. While the estimated ground resolution of the S190B at low contrast was approximately 21 meters (70 feet), this high contrast target of 12.5 meters (38 feet) shows up quite vividly. From the logs, it could further be established that boats less than 8.9 m (27 feet) could not be seen.

S191 System

The S191 sensor is made up of three major elements - a Cassegrainian telescope and plane-mirror optical system that provided an image of the scene to the other two elements, a filter-wheel spectrometer that scanned the radiation from the scene and a boresighted viewfinder and tracking system with the same line of sight as the spectrometer. The infrared sensor's instantaneous field of view was approximately .435 kilometers (.235 nautical mile) in diameter. Incoming radiation was split into short and long-wavelength bands; 0.4 to 2.5 micrometers and 6.6 to 16 micrometers.

Examination of the S191 data acquired over the test area during the Skylab/Gamefish Experiment has revealed that cloud cover obscured major portions of the sensor's coverage along the flight track. This is shown in the S190A station 6 (0.5 - 0.6 µm) imagery with the test site and S191 ground track superimposed. (Figure 14). An isometric presentation of the data from the short wave band (0.4 to 1.1 µm) of the S191 sensor is shown in Figure 18. This presentation of the data

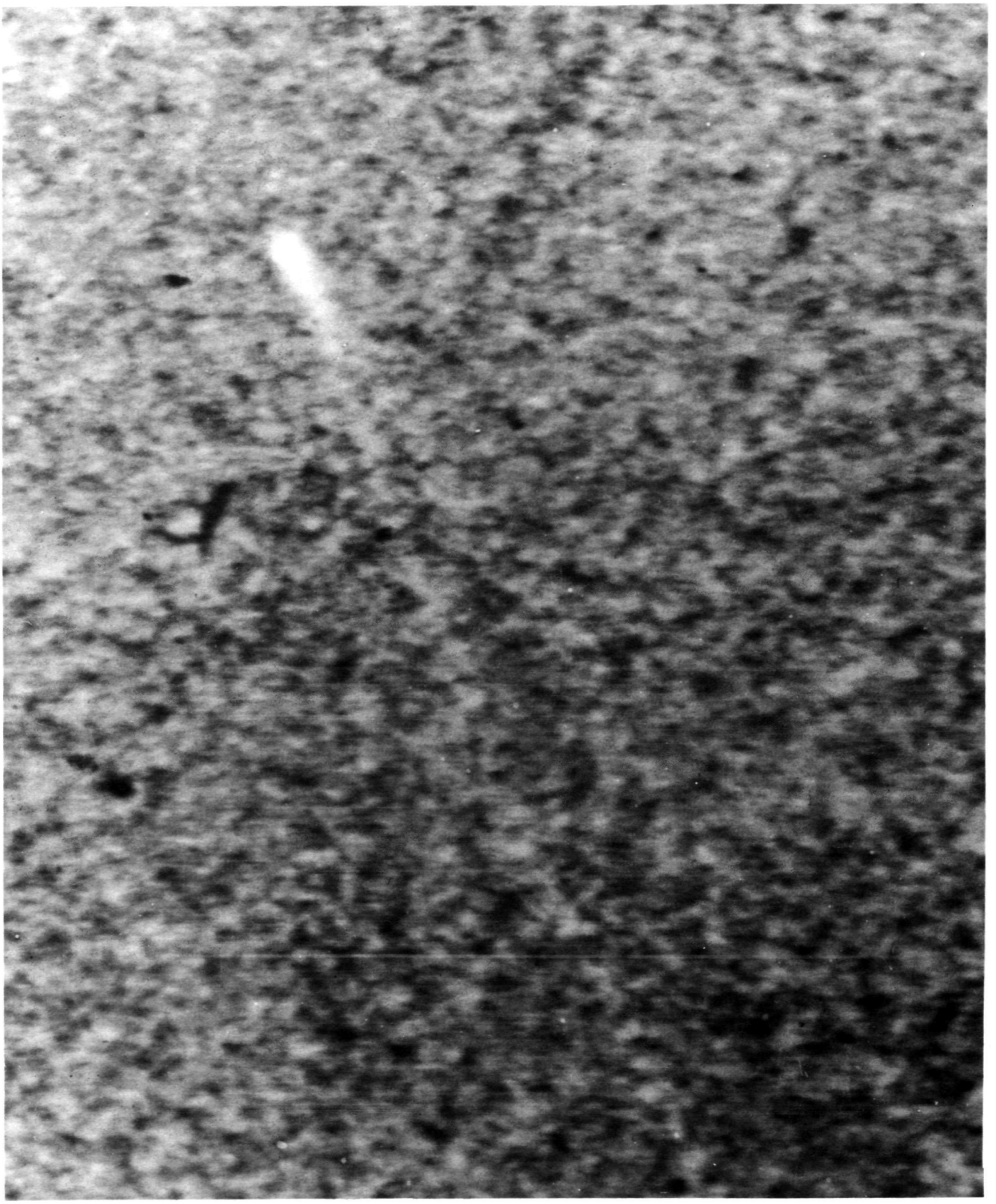

Figure 17. S190 Photograph of Sport Fishing Vessel Magnified 50 Times

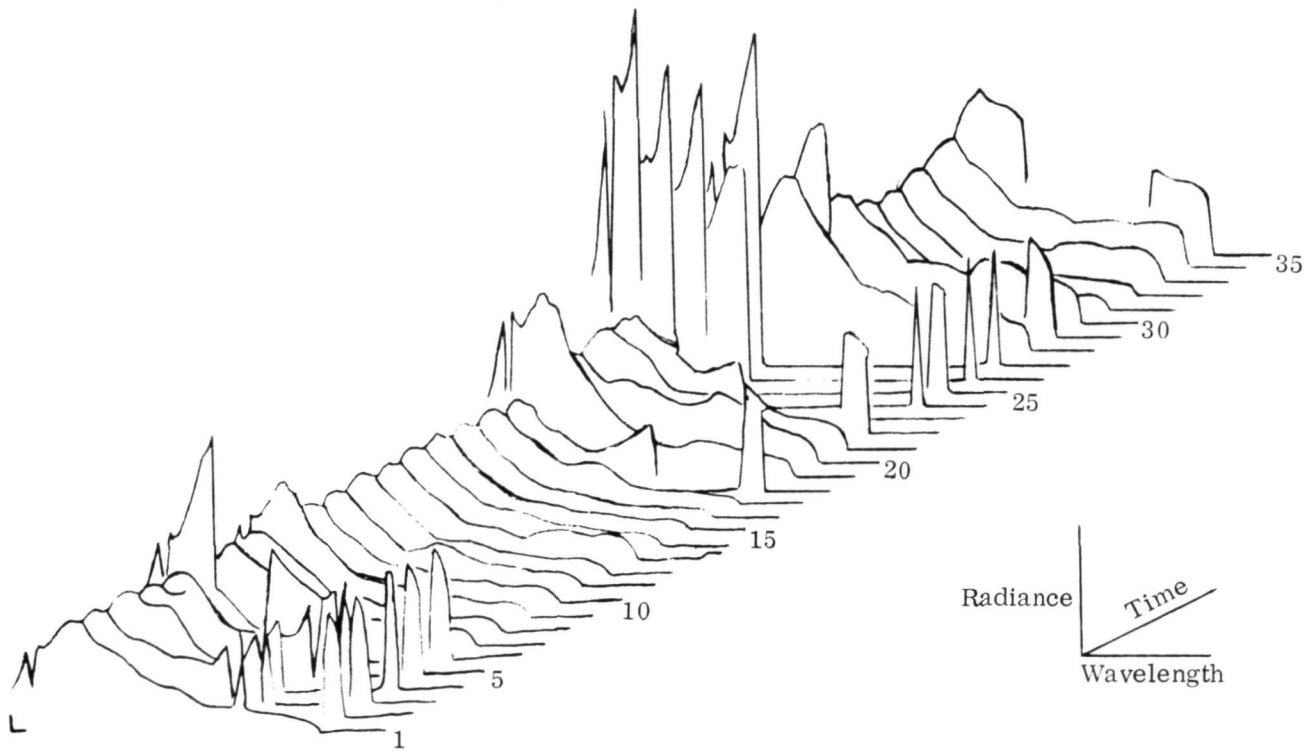

Figure 18. The Isometric Presentation of the Visible Portion of the S191 Spectra

represents the information from channel A3, the high gain silicon detector. When the channel saturates, a value of zero is indicated, so when the spectrometer was viewing the very bright clouds and the signal was saturated, the spectrum indicates a zero radiance. Spectra 13 through 35 were taken very near or over the test area. Surface sampling stations were located in areas sampled by the S191 as spectra 13, 15, 18, 20, 22, 25, and 27. Spectra 13 through 15 were cloud free, while spectrum 18 indicates saturation in one portion of the spectrum, due most likely to a small cloud which entered the sensor field of view only briefly. Spectra 19 through 21 appear contaminated, but not saturated. Spectra 22 through 27 are saturated. The rest of the spectra are all contaminated. This limited set of sensor data has prevented further analysis such as development of predictive algorithms for chlorophyll-a and turbidity based on selected S191 spectra.

In addition, initial plans to compute radiance values every 50 nanometers from 0.4 to 0.7 µm range for each 8.05 km (5 mile) subsquare crossed by the S191 flight track resulted in data for only one subsquare. This prohibited any type of statistical analysis between the white marlin distribution and data from this sensor.

S192 Multispectral Scanner

The multispectral scanner was an optical electromechanical scanner which collected incoming radiant energy using a rotating mirror in the image plane to conically scan the scene viewed. The energy scanned in the image plane passed through a reflective Schmidt corrector mirror and through a field stop that was the entrance slit of a prism spectrometer. The short wavelengths (0.41 to 2.43 micrometers) were separated from the long thermal wavelength band (10.2 to 12.5 micrometers) by a dichroic mirror. The spectrally dispersed electromagnetic energy received from the scene irradiated thirteen detectors simultaneously. Detectors and associated wavelengths are listed below:

Band No.	Wavelength, Micrometers
1	0.41 - 0.45
2	0.44 - 0.52
3	0.49 - 0.56
4	0.53 - 0.61
5	0.59 - 0.67
6	0.64 - 0.76
7	0.75 - 0.90
8	0.90 - 1.08
9	1.00 - 1.24
10	1.10 - 1.35
11	1.48 - 1.85
12	2.00 - 2.43
13	10.20 - 12.50

Each detector produced an electronic signal that corresponded to the average value of the radiance received in its spectral band from the spot on the surface in the instrument's 0.182 milliradian field of view. The field of view of each detector provided an instantaneous square ground coverage of 79 meters (260 feet) swept in a conical scan. The ground swath width of the sensor was 74 kilometers (40 nautical miles).

Black and white 12.7 centimeter (5-inch) film images of corrected/filtered data from bands 1-13

and digital data on tapes from bands 1-9 and 13 have been received from NASA-JSC. Evaluation of the S192 imagery resulted in the identification of a ringing of cloud edges across the cloud free areas of the imagery in bands 3, 4, 5, and 8. Discussions with NASA have confirmed that the high frequency filtering of the data created this distortion as shown in Figure 19. Distortion can be seen on both sides of the shoreline as waves and out further in the frame as cloud edge duplication. Band 2 is very noisy with frequent scan line dropout. Band 13 is also very noisy.

A request to reprocess bands 1-9, and 13 without high frequency filtering in bands 1-5, 7 and 8 has been submitted to the NASA. Further analysis of this set of data is pending receipt of data.

PREDICTION MODELS

Model Development

Multiple regression analysis was used to develop models to predict white marlin distribution ($\bar{D}$) in the Skylab test area. Initial runs utilized the eleven parameters listed in Table IV along with all possible interactions (formed by computing the products of each parameter pair) as the independent parameters. The first models D_1, D_2, D_3 listed in Table VI were constructed utilizing data collected on 4 August, on 5 August, and the combination of 4-5 August. These models were developed based on five parameters: surface water temperature (T), Secchi extinction depth (C), salinity (S) and the two interaction parameters, the product of Secchi extinction depth and chlorophyll-a, (CA), and the product of salinity and surface water temperature (ST). Comparison of constant terms and coefficients (by magnitude and sign) in models D_1, D_2, and D_3 reveal extreme difference or instability from day to day. Therefore, it appeared that important information was not considered, a combination of linear terms was not sufficient to model the day to day changes, or a white marlin distribution model could not be developed.

Additional work was initiated to try to stabilize the models. Water density was computed and substituted for the product of water temperature and salinity. The latter two had been used in the earlier regression runs. A measure of water density (σ_t) was computed utilizing the following equations (21).

$$C1 = \frac{S-0.030}{1.805} \qquad \text{(d)}$$

$$\sigma_o = -0.069 + 1.4708\ C1 - (1.57 \times 10^{-3})\ C1^2 + (3.98 \times 10^{-5})\ C1^3 \qquad \text{(e)}$$

$$\Sigma_t = -\frac{(t-3.98)^2}{503.57} \cdot \frac{t+283}{t+67.26} \qquad \text{(f)}$$

$$A_t = t\left[4.7867 - 0.098185t + (1.0843 \times 10^{-3})t^2\right] \times 10^{-3} \qquad \text{(g)}$$

$$B_t = t\ (18.03 - 0.8164t + 0.01667t^2) \times 10^{-6} \qquad \text{(h)}$$

$$\sigma t = \Sigma_t + (\sigma_o + 0.1324)\left[1 - A_t + B_t\ (\sigma_o - 0.1324)\right] \qquad \text{(i)}$$

where: S = salinity in $^{o}/oo$
t = temperature in ^{o}C
σ_t = density parameter

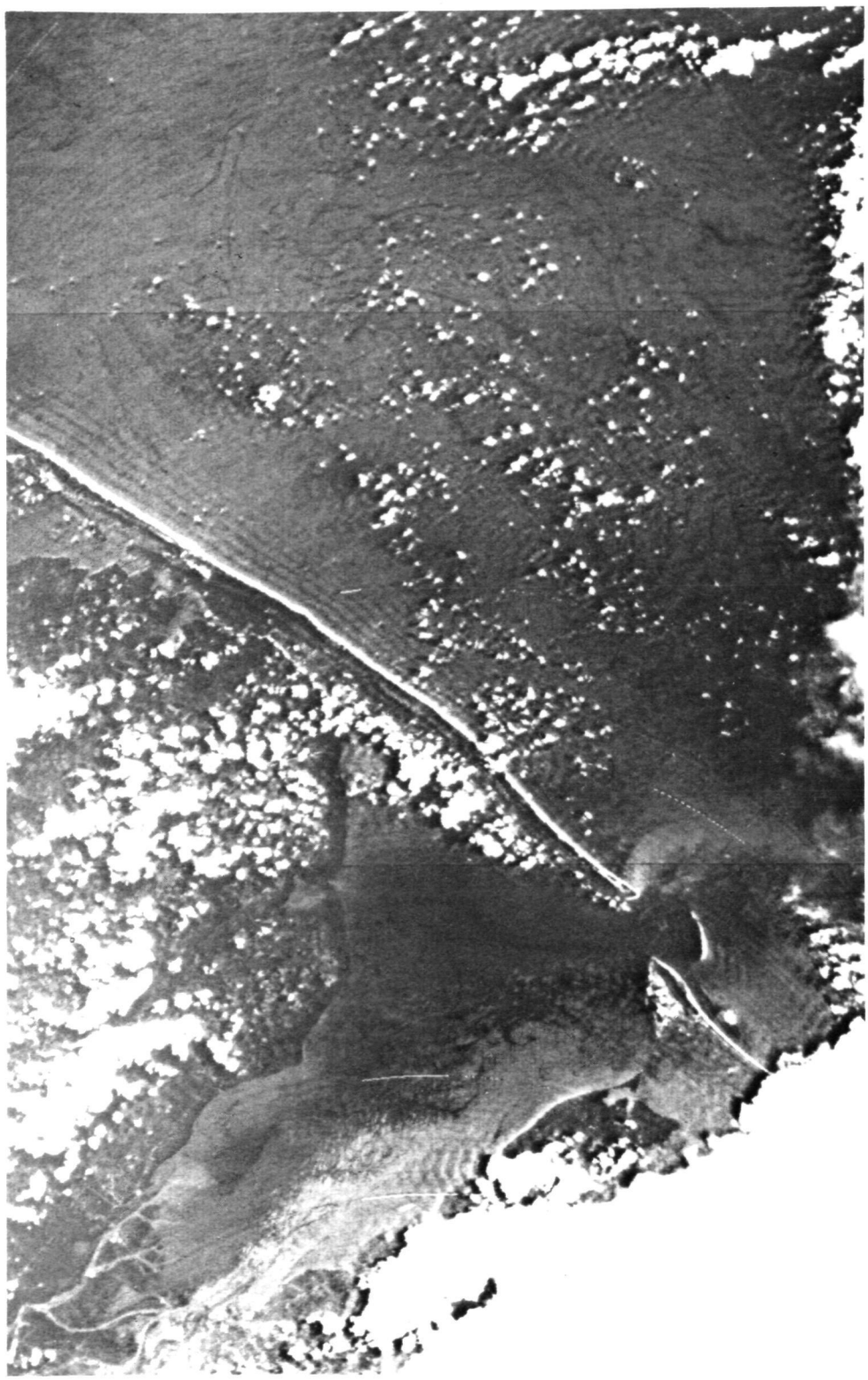

Figure 19. Imagery of Part of the Test Area Taken from Band 3 of the S192 System

TABLE VI. EMPIRICAL REGRESSION MODELS WHICH PREDICT WHITE MARLIN (D) IN THE SKYLAB TEST AREA

T = Water temperature (°C)
C = Secchi disc transparency (m)
S = Salinity (ppt)
ST, CA = Interaction formed as the product of the respective parameters

B = σ_t (measure of water density)
where $\sigma_t \times 10^{-3} + 1$ = water density (g/cm^3)

A = Chlorophyll-a (mg/m^3)

MODEL	INCLUSIVE DATES (1973)	n	REGRESSION MODEL	STANDARD ERROR OF $\bar{D}$	MODEL CORRELATION COEFFICIENT	SIGNIFICANCE LEVEL (%)
D_1	4 August	24	$\bar{D}$ = -419.5394 + 14.3929T +12.9764S + .0567C -.4461ST + .0074CA	0.3435	0.797	99.5
D_2	5 August	22	$\bar{D}$ = 164.1002 - 5.3527T -6.3246S + 0.173C +.2071ST - .0021C	0.4996	0.499	50
D_3	4 & 5 August	46	$\bar{D}$ = -25.4052 + .9301T +.3258S + .0139C -.0133ST + .0008CA	0.4751	0.436	75
D_4	4 August	24	$\bar{D}$ = -13.3676 + .6583T +.0718C + .3651B +.0043CA	0.3589	0.762	99.5
D_5	5 August	22	$\bar{D}$ = -22.4714 + .8179T +.0143C -.1035B -.0014CA	0.4879	0.489	60
D_6	4 & 5 August	46	$\bar{D}$ = -12.8553 + .4959T +.0142C - .0950B +.0007CA	0.4693	0.436	90

NOTE: Water density (g/cm^3) at observed salinity temperature and 0 meters depth (atmospheric pressure) = $\sigma_t \times 10^{-3} + 1$.

The resulting density measure σ_t was used in constructing models D_4, D_5 and D_6 which also contain surface water temperature, Secchi extinction depth, and the product of Secchi extinction depth and chlorophyll-a. Comparison of the constant term and coefficients reveals a significant improvement in the stability of coefficient of each parameter from model to model. It should also be noted that the significance level was improved on models D_5 and D_6. The result indicates that the relationship between white marlin distribution and the environmental parameters is more complex than a linear combination of the environmental parameters. However, while only two days of data were available for modeling efforts, it is evident that the relationship can be modeled with reasonable stability from day to day.

Model Evaluation

The D_4 and D_5 models were tested with independent test data by using 4 August test data in D_5 (developed from 5 August data) and 5 August test data in D_4 (developed from August 4 data). In each case the resulting unnormalized predicted distribution values (Y) were separated into low, medium, and high probability ranges. This was accomplished by computing the mean ($\bar{Y}$) and standard deviation (S) of each set of predicted values. The probability ranges were fixed as follows:

$$\text{Low probability} = Y < \bar{Y} - 1/2\ S$$

$$\text{Medium probability} = \bar{Y} - 1/2\ S \leq Y \leq \bar{Y} + 1/2\ S$$

$$\text{High probability} = Y > \bar{Y} + 1/2\ S$$

Each predicted value for each test square was classified as low, medium, or high depending on the probability range in which it fell. The actual distribution value for each test square was assigned a high probability if it had a distribution value of 1 and a low probability if it had a distribution value of 0.

Nine of 24 fishing squares were classified as medium probability areas. Actual fish catch in those nine squares revealed that there existed a 50 percent chance of being in an area that had fish. Considering the extreme of low and high probability regions for model evaluation as shown in Table VII, the model was 93 percent accurate in predicting fish location in the remaining 15 squares.

TABLE VII. EVALUATION SUMMARY FOR 4 AUGUST PREDICTED VALUES USING MODEL D_5

Actual	Predicted	Number of Test Squares
HIGH	HIGH	5
LOW	LOW	9 = 93% correct
LOW	HIGH	1
HIGH	LOW	0 = 7% incorrect

Ten of the 24 squares fished produced fish-catch results which revealed that a fisherman had a 42 percent chance of being in a location having fish if a square was randomly selected from the 24 squares. However, if a fisherman selected one of the six predicted high probability squares his chance of being in area having fish increased to 83 percent.

To further determine the value of the predicted high probability squares, an evaluation of these squares with associated abundance data was made. It was found that in the six squares selected by Model D_5 from 4 August data or 25 % of the test area, 67% of the white marlin were hooked in 31% of the fishing time.

Visual representations of the predicted values from model D_5 is shown in Figure 20. The number of predicted test squares within a given range having fish are denoted by the shaded areas or solid lines. The number of predicted test squares within a given range not having fish are denoted by the dash lines. Ideally the shaded areas should cluster near the high value or high probability portion of range and the dash line areas near the low value or low probability portion with a very minimum of intersection. The results shown in Figure 20 tend toward the ideal conditions.

The analysis of 4 August data utilizing model D_5 demonstrates the potential for reducing a fishing area by identifying high probability areas. For the cases in point a factor of three or four would be achieved. Furthermore, by only considering high probability areas, the overall probability of being in an area where fish may be hooked, can be increased approximately by a factor of two in the case discussed.

MODEL TESTING OF AIRCRAFT REMOTELY SENSED DATA

Data values for remotely sensed sea surface temperature, chlorophyll-a and turbidity were selected from the applicable contour maps. No remotely inferred values for salinity were available so sea truth salinity measurements were used. Water density was computed for each square using remotely sensed temperature and the sea truth salinity. The data values were substituted in Model D_5 and the predicted white marlin distribution values which resulted, were classified as low, medium or high probability areas according to the procedure given in Model Evaluation. Again, not considering the predicted medium probability squares (8 in number) the resulting evaluation is shown in Table VIII. The results are probably indicative of errors occurring in one or more of the following processes.

- Selection of data from hand contoured charts of remotely sensed data.
- Use of actual distribution comparison values based over the entire day rather than the plus or minus two hours of the aircraft flight time.
- Extrapolation of values from the narrow footprint coverage of the aircraft sensors.

TABLE VIII. EVALUATION SUMMARY FOR 5 AUGUST PREDICTED VALUES USING MODEL D_5 WITH REMOTELY SENSED VALUES

Actual	Predicted	Number of Test Squares
LOW HIGH	LOW HIGH	2 1 = 50% correct
LOW HIGH	HIGH LOW	2 1 = 50% incorrect

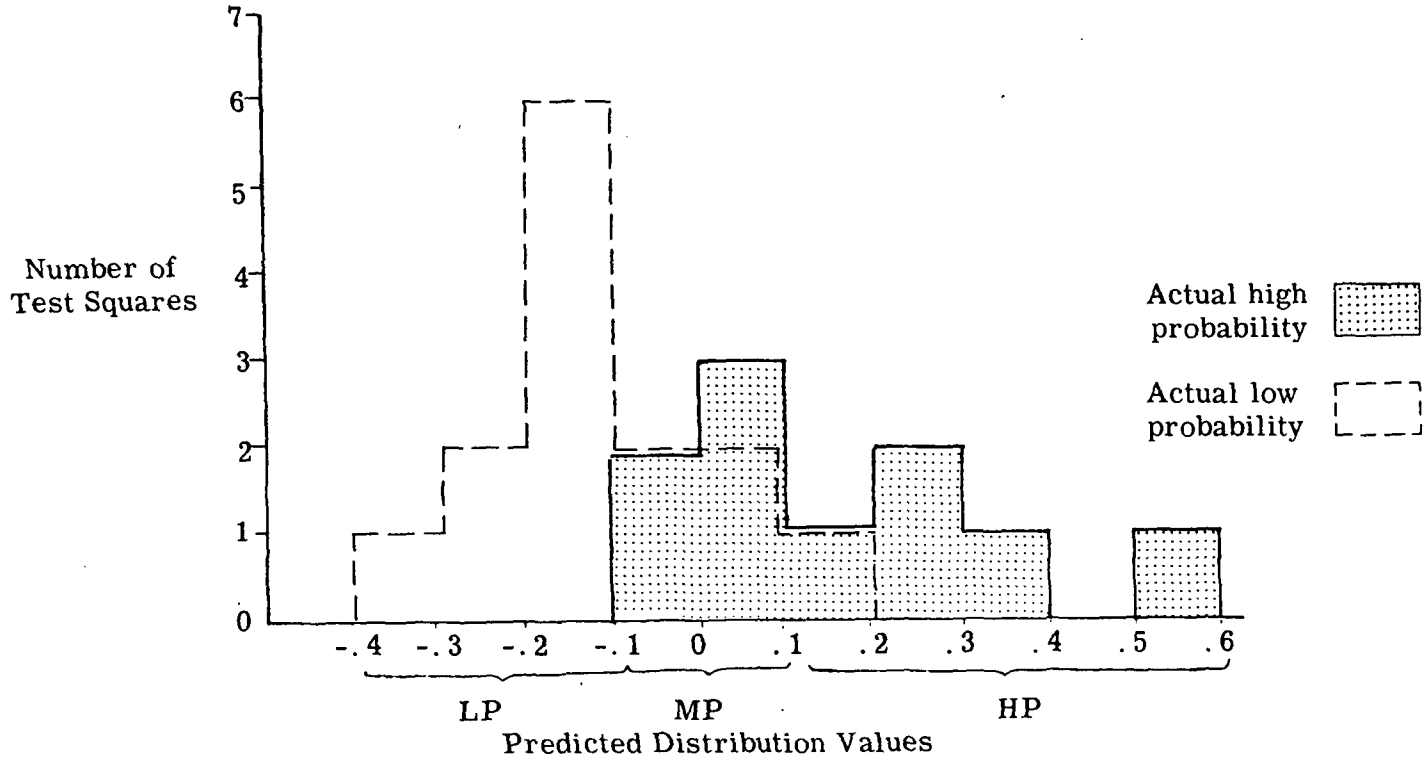

Figure 20. Evaluation of August 4 Predictions, Using August 5 Model D_5

Application

Oceanic gamefish distribution prediction models of the type reported herein would clearly serve sportsfishermen and resource managers. Knowledge of highest potential catch areas as a function of time will provide sportsfishermen with the benefits of increased catch and decreased time and fuel expenditures. Figure 21 is an example of a prediction model product which displays fishing areas in terms of catch potential.

These prediction models are presently not adequate for resource management applications. Daily operational utilization of these models must wait until techniques for remotely sensing the necessary environmental parameters become fully functional on a synoptic basis.

As models are improved to an acceptable precision level and as repetitive data acquisition becomes economically feasible, it is reasonable to presume that these or similar models could provide the abundance and distribution information necessary for development of conservation and harvesting procedures. As operational readiness and confidence in such models are established, resource managers would have additional information on which to base domestic and international conservation decisions.

Application to Wide Areas

Considerations relative to the application of the model to wide areas may be categorized as both spatial and temporal. The parameters used in the model were selected because they applied significantly to the white marlin resource in the Gulf of Mexico during the time frame of data acquisition. Elsewhere in the world, for other species and possibly different time frames, other parameters might figure more importantly. The models would require rework using the parameters most applicable to the particular area or possibly using the same set with additional parameters representing the unique, environmental characteristics identified with that area.

The relatively narrow range of values used in model development is another factor presently limiting use elsewhere except where the environment is analogous to that of the Gulf of Mexico during the month of August. For example, the sea truth measurement of sea surface temperature varied from 28.5°C to 31.6°C during the data acquisition operations. For temperature values outside that narrow band, it is unclear if the model performance would be adequate. This is true about each parameter.

The models are based on data taken during the limited, two day operations and which covered a very small portion of the total range of each parameter. It is questionable how well the model would function with data outside the range of the data with which it was developed. However, since parameter range is obviously associated with seasonal weather (except in the tropics), model inadequacy with respect to data range may be considered a temporal deficiency which could be corrected by the input of additional data collected during other seasons of the year.

The model could be tested elsewhere than in the Gulf of Mexico to resolve the question of spatial deficiency. For example, white marlin are fished quite heavily along the southern Atlantic Coast which could be used as second test area from which to collect data. Future investigations could well include both temporal and spatial testing of the relationship between white marlin and the environment.

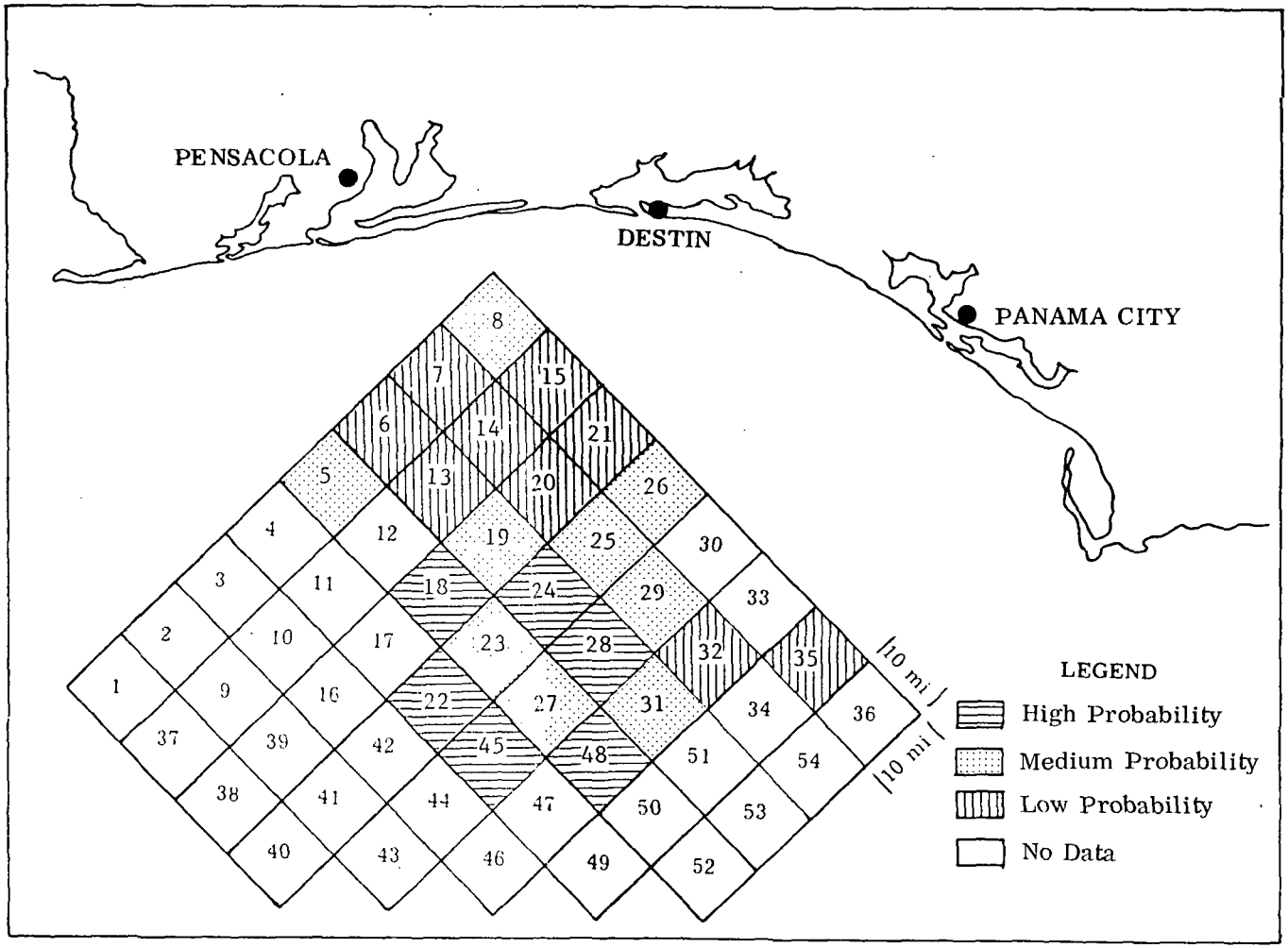

Figure 21. Prediction Results of August 4 Data Using Model D_5

CONCLUSIONS

The distribution and abundance of white marlin correlated with sea truth measurements. Correlation analyses were also done for dolphin, but the results were inconclusive.

Prediction models for white marlin were developed which demonstrated a potential for increasing the probability of game-fishing success. They also demonstrated a potential for reducing a sportsman's search time significantly by identifying areas which have a high probability of being productive.

Chlorophyll-a, sea surface temperature and turbidity (Secchi extinction depth) values were inferred from aircraft sensor data. Comparisons with sea truth measurements indicate that, in spite of sometimes unfavorable atmospheric conditions, reasonable accuracy can be expected.

Cloud cover and sun-glint in the test area on August 5, 1973, inhibited the usefulness of the Skylab S190A and S190B imagery. The S190A and S190B imagery was density sliced/colored enhanced with white marlin location superimposed on the image, but no density/white marlin relationship could be established. The resolution of the S190B system was sufficient to see fishing boats 12.5 meters (38 feet) in length. This demonstrated a potential use in fishery remote sensing surveillance systems. S191 data are insufficient for detailed fishery analysis. The S192 multispectral data were evaluated and a significant problem associated with high frequency filtering was identified. Detail analysis of these data, with respect to the fishery resource data, was delayed until this problem can be corrected. Because of these factors, it remains unclear if data from satellite sensors can be used in models to predict gamefish abundance and distribution. However, with the successful identification of the fisheries significant oceanographic parameters and the demonstration of the capability of measuring most of these parameters remotely, the first step toward establishing the feasibility of utilizing remotely sensed data to assess and monitor the distribution of oceanic gamefish was accomplished.

ACKNOWLEDGEMENTS

The Skylab Oceanic Gamefish Project was a lengthy, multidisciplined experiment entailing an extensive data gathering operation followed by a complex and detailed data analysis phase. In any such experiment it is difficult to focus on individual efforts. However, each role was important and the Principal Investigator gratefully acknowledges the efforts of the many participating organizations and individuals who contributed to the experiment.

Sportsfishermen provided gamefish data resulting from participation in a tournament coordinated through the Pensacola Big Game Fishing Club by a committee of anglers representing four big gamefishing clubs and two charterboat associations. The committee members were Mr. G. Arnold III, Mobile Big Game Fishing Club, Mr. Bill Bacon, Destin Charter Boat Association, Mr. M. Claverie, Jr., New Orleans and Golden Meadow Big Game Fishing Clubs, Dr. F. T. Neth, Pensacola Big Game Fishing Club and Mr. B. J. Putnam, Panama City Charter Boat Association. Another contribution from the sportsfishing community was the use of facilities at check point marinas at Pensacola, Destin and Panama City, FL, during field operations.

The National Aeronautics and Space Administration's (NASA) Lyndon B. Johnson Space Center (JSC), Houston, TX, directed the activities of the Skylab astronauts during overpass, provided the earth survey aircraft, the NC130B, to overfly the test site, and contracted the experiment. The NASA National Space Technology Laboratory (NSTL), Bay St. Louis, MS, provided extensive laboratory, field site and public relations support. The NASA contractors at NSTL, the General Electric Company and Lockheed Electronics, Inc., assisted with field and technical support.

The NASA JSC Earth Resources Laboratory (ERL) located at the NSTL was responsible for the planning, acquisition and processing of surface and remote oceanographic data. Mr. E. L. Tilton, NASA ERL, and his successor as technical monitor, Dr. G. C. Thomann, provided guidance. Mr. J. W. Weldon, now NASA JSC, as a co-investigator did much of the operational planning and execution with Mr. K. Faller, NASA ERL, assuming the responsibilities of Mr. Weldon after the latter's departure. Mr. Faller has contributed significantly to the analysis segment of the experiment in the area of remotely sensed oceanographic data correlation to the environment.

The U.S. Air Force provided DAPS satellite data received at Keesler AFB, MS, and a U.S. Navy representative from the Environmental Prediction Research Facility, Monterey, CA, assisted in the analysis of the DAPS data. Weather data was also received through the National Environmental Satellite Service from the NOAA-2 satellite. The weather station at Eglin AFB, FL, launched a special radiosonde coincident with Skylab overpass to provide meteorological data.

Test site safety measures were coordinated with the U.S. Naval Air Station, Pensacola, FL, and the U.S. Coast Guard Headquarters at Mobile, AL. The Coast Guard Station on Santa Rosa Island, FL, provided logistics support during field operations.

The National Oceanic and Atmospheric Administration's (NOAA) National Marine Fisheries Services (NMFS) laboratories at NSTL, Pascagoula, MS, Panama City, FL, and the Southeast Fisheries Center (SEFC), Miami, FL, provided management and technical direction for the experiment. Mr. W. H. Stevenson, now at NMFS Southeast Regional Office, St. Petersburg, FL. organized and managed the experiment as the initial Principal Investigator at the NMFS Fisheries Engineering Laboratory (FEL) at NSTL. Mr. E. J. Pastula, Jr., NMFS FEL, as a co-investigator, contributed to operations and data analysis. Mr. P. C. Cook, NMFS FEL, exercised budgetary control throughout the experiment. Mr. L. Rivas, NMFS Panama City, provided technical guidance on oceanic gamefishing and also functioned as a liaison with gamefishing sportsmen and charterboat captains. Mr. E. G. Woods, NMFS FEL, planned and coordinated field operations on 4-5 August.

REFERENCES

1. Woods, E. G. and Cook, P. C., 1973: Skylab Oceanic Gamefish Project. International Gamefish Research Conference, 73 pp.

2. Savastano, K; Pastula E. Jr.; Woods G.; Faller, K.; Preliminary Results of Fisheries Investigation Associated with Skylab-3.

3. Faller, K. H., 1974: Remote Sensing of Oceanic Parameters During the Skylab/Gamefish Experiment.

4. Fox, W. W., 1971: Temporal-Spatial Relationships among Tunas and Billfishes Based on the Japanese Longline Fishery in the Atlantic Ocean 1956-1965. Sea Grant Tech. Bulletin No. 12, 77 pp.

5. Kemmerer, A. J., Benigno, J. A., Reese, G. B., and Minkler, F. C., 1973: A Summary of Selected Early Results from the ERTS-1 Menhaden Experiment, NASA CR-133152, 37 pp.

6. Wise, J. P. and Davis, C. W., 1973: Seasonal Distribution of Tunas and Billfishes in the Atlantic. NOAA Technical Report NMFS SSRF-662, 24 pp.

7. Gibbs, R. H., Jr., 1957: Preliminary Analyses of the Distribution of White Marlin, Makaira albida (Poey), in the Gulf of Mexico. Bulletin of Marine Science of the Gulf and Caribbean 7-(4) 10 pp.

8. Gulf of Mexico Its Origin, Waters, and Marine Life. Fishery Bulletin 89, Vol. 55, 1954, 601 pp.

9. De Sylva, D. P. and Davis, W. P., 1963: White Marlin, Tetrapturus albidus, in the Middle Atlantic Bight, with Observations on the Hydrography of the Fishing Grounds, Copeia, No. 1, 18 pp.

10. Daughtrey, K. R. 1973: Techniques and Procedures for Quantitative Surface Water Temperature Surveys using Airborne Sensors. Earth Resources Laboratory, Report 80, Mississippi Test Facility, 30 pp.

11. Worthington, H. T., 1973: Remote Measurement of Surface Water Temperatures in Coastal Waters, NASA Earth Resources Laboratory, Report 85, Mississippi Test Facility, 33 pp.

12. Boudreau, R. D., 1972a: A Radiation Model for Calculating Atmospheric Corrections to Remotely Sensed Infrared Measurements. NASA Earth Resources Laboratory Report 14, Mississippi Test Facility, 71 pp.

13. Boudreau, R. D., 1972b: Correcting Airborne Scanning Infrared Radiometer Measurements for Atmospheric Effects. NASA Earth Resources Laboratory Report 29, Mississippi Test Facility, 34 pp.

14. Worthington, H. T., 1974: Personal Communication.

15. Weldon, J. W., 1973: Remote Measurement of Water Color in Coastal Waters, NASA Earth Resources Laboratory, Report 83, Mississippi Test Facility, 47 pp.

16. Clark, G. L., Ewing, G., and Lorenzen, C., 1970: Spectra of Backscattered Light from the Sea Obtained from Aircraft as a Measure of Chlorophyll Concentration. Science, 67, pp 1119-1121.

17. Hovis, W. A., Forman, M. L., and Blaine, L. R., 1973: Detection of Ocean Color Changes from High Altitude, Goddard Space Flight Center Internal Technical Memorandum TMX-70559, 25 pp.

18. Jones, J. B., 1973: Determination of Chlorophyll Content of Water. Lockheed Electronics Corporation, Technical Memorandum DATM-061, Mississippi Test Facility, 7 pp.

19. Thomann, G. C., 1973: Remote Measurement of Salinity in an Estuarine Environment, Remote Sensing of Environment 2, 249 pp.

20. McClain, E. P. and Strong, A. E., 1969: On Anomalous Dark Patches In Satellite-Viewed Sunglint Areas, Monthly Weather Review, Vol 97, No. 12, pp 875-884.

21. Knudsen, M., 1962: The Determination of Chlorinity by the Knudsen Method, Reprint by G. M. Manufacturing Company, 63 p.

BIBLIOGRAPHY

Ostle, B., 1963: Statistics in Research, Second edition, The Iowa State University Press, 585 pp.

Stevenson, W. H. and Pastula, E. J., Jr., 1973: Investigation Using Data from ERTS-1 to Develop and Implement Utilization of Living Marine Resources, Final Report, Mississippi Test Facility, Bay St. Louis, Mississippi, 185 pp.

Spiegel, M. R., 1961: Schaum's Outline of Theory and Problems of Statistics, McGraw-Hill, 359 pp.

Yentsch, C. S., 1960: The Influence of Phytoplankton on the Color of Sea Water, Deep-Sea Research, Vol. 7, p. 1.

Skylab Earth Resources Data Catalog: NASA Lyndon B. Johnson Space Center, Houston, Texas.